探討突變基因 DCX 在大腦神經發育和平腦症中的影響

Subcellular Roles of DCX Mutations in Brain Development and Lissencephaly

研究生：林均儒 (Jun-Ru Lin)

指導教授：蔡金吾 博士 (Jin-Wu Tsai, Ph.D.)

國立陽明大學

腦科學研究所

碩 士 論 文

Institute of Brain Science

National Yang-Ming University

中華民國一〇九年六月

June, 2020

國家圖書館學位論文延後公開申請書

編號：

Application for Embargo of Thesis/Dissertation

申請日期：民國 109 年 06 月 16 日

Application Date: 2020 / 06 / 16 (YYYY/MM/DD)

申請人姓名 Applicant Name	林均儒	學位類別 Graduate Degree	■碩士 Master □博士 Doctor	畢業年月 Graduation Date (YYYY/MM)	民國 109 年 06 月 2020 / 06
學校名稱 University	國立陽明大學 National Yang-Ming University		系所名稱 School/Department	腦科學研究所 Institute of Brain Science	
論文名稱 Thesis / Dissertation Title	探討突變基因 DCX 在大腦神經發育和平腦症中的影響 Subcellular Roles of DCX Mutations in Brain Development and Lissencephaly				
延後公開原因 Reason for embargo	□申請專利並檢附證明，專利申請案號： Filing for patent registration. Registration number: ■準備以上列論文投稿 Submission for publication. □涉及國家機密 Contains information pertaining to the national secret. □依法不得提供，請說明： Withheld according to the law. Please specify.			公開日期 Delayed Until	民國 114 年 06 月 16 日 2025 / 06 / 16 (YYYY/MM/DD)

申請人簽名：
Applicant Signature: 林均儒

指導教授簽名：
Advisor Signature: 彭秀玉

學校認定/審議單位章戳：
Seal of the Authorization Institute (國立陽明大學系/所章戳 Seal of the Department/Institute of NYMU)

國立陽明大學 腦科學研究所 Institute of Brain Science NATIONAL YANG-MING UNIVERSITY

【說明】

1. 以上所有欄位請據實填寫並檢附證明文件，由學校向本館提出申請，缺項或簽章不全，恕不受理。
2. 論文尚未送交國家圖書館，請於提送論文時，夾附親筆簽名申請書1份。
3. 論文已送達國家圖書館，請將親筆簽名申請書一式2份掛號郵寄10001臺北市中山南路20號國家圖書館館藏發展及書目管理組，並於信封註明「學位論文延後公開申請書」。
4. 送交陽明大學圖書館之學位論文，請將本申請書影本裝訂於紙本論文書名頁之次頁，另備影本於辦理離校時交予圖書館。

【Notes】

1. Please fill in all blanks and deliver to your university. The application form will not be accepted for processing until all information, signatures, and stamps are included.
2. If the thesis or dissertation is not yet submitted to the NCL, please attach the signed application form to the thesis or dissertation.
3. If the thesis or dissertation has been submitted to the NCL, please send a registered letter with 2 copies of the signed application form attached. The letter should be addressed to "Collection Development Division", National Central Library with a note in the envelope indicating "Application for delay of public release" to the following address. No.20, Zhongshan S. Rd., Zhongzheng District, Taipei City 10001, Taiwan (R.O.C.)
4. The copy of application form should be attached and bind in thesis/dissertation submitted to NYMU Library.

(以下由國圖填寫 For Internal Use)

承辦單位_館藏組：_____ 日期/處理狀況：

典藏地：_____ 登錄號：_____ 索書號：

會辦單位_知服組：_____ 日期：_____ □移送並註記，原上架日期：

論文系統：_____ 日期：

國立陽明大學 碩士學位論文審定同意書

腦科學 研究所 林均儒 君（學號：30502009）

所提之論文

題目：（中文）探討突變基因 DCX 在大腦神經發育和平腦症中的影響

（英文）Subcellular Roles of DCX Mutations in Brain Development and Lissencephaly

經學位考試委員會審查通過，特此證明。

學位考試委員會（簽名） 召集人 楊定一

口試委員

劉祐岑

蔡金吉

☑論文已完成修改及論文原創性比對

指導教授 蔡金吉（簽名）

所　　長 楊定一（簽名）

中華民國 109 年 6 月 11 日

109.05 版

國立陽明大學學位論文電子檔授權書

〖請將影本裝訂於紙本論文書名頁後〗

本授權書所授權之學位論文全文電子檔，為本人於國立陽明大學腦科學研究所基礎腦科學組，108學年度第2學期取得碩士學位之論文。

論文題目：探討突變基因DCX在大腦神經發育和平腦症中的影響
指導教授：蔡金吾

■ 同意

本人茲將本著作，以非專屬、無償授權國立陽明大學與台灣聯合大學系統圖書館：基於推動讀者間「資源共享、互惠合作」之理念，及回饋社會與學術研究之目的，國立陽明大學及台灣聯合大學系統圖書館得不限地域、時間與次數，以紙本、光碟或數位化等各種方法收錄、重製與利用；於著作權法合理使用範圍內，讀者得進行線上檢索、閱讀、下載或列印。

論文全文電子檔之公開網域範圍及時間：

校內區域網路	■ 中華民國 114 年 6 月 16 日公開
台灣聯合大學網際網路	■ 中華民國 114 年 6 月 16 日公開
校外網際網路	■ 中華民國 114 年 6 月 16 日公開

■ **同意全文電子檔送交國家圖書館**

授權國圖公開閱覽日期	■ 中華民國 114 年 6 月 16 日公開

授 權 人：林均儒

親筆簽名： 林均儒

指導教授簽名： 蔡金吾

中華民國 109 **年** 6 **月** 16 **日**

本研究榮獲財團法人罕見疾病基金會
「第21屆罕見疾病博碩士論文獎助學金」獎助
謹於此特別致謝

誌謝 Acknowledgement

如果說每次的相遇不是偶然，而是因為每一次的決心累積而來，那我很感謝有這些機會讓我可以來到這裡。回首過去經歷過的種種，感覺已經離我好遠好遠，有些剛來的記憶已經模糊，有些刻苦銘心，不過一路跌跌撞撞也算是撐過了這幾年。

實驗室還有腦科所是另一個避風港，每天都有很多有趣又笑不完的事情，沒有想過碩班可以再辦像是工作坊或甚至是跟醫學院的所有師生一起完成畢業影片，我以為這些都是大學的事了。才發現學校除了是學術殿堂外，這裡也像個遊樂園，只要有個好點子，老師都很願意給學生機會去嘗試不同的可能，覺得自己很幸運可以在這裡。所以特別感謝蔡老師，讓我加入他的實驗室，也讓我試著從頭開始一個新的題目，雖然剛開始很徬徨，但當老師讓我自己挑幾個喜歡的基因來做為碩班的題目時，心裡滿是覺得不可思議。很謝謝老師讓我感受到研究自由，而且每次遇到困難的時候，老師每次都會突然講了幾句很關鍵的話，然後事情就順順的走下去了(不知道是怎麼辦到的)。除了學業上，也很感謝老師給我很多人生的建議，點破了很多我沒看到的東西，還好當初有跑來找老師問你可不可以當你的學生，希望沒有給老師太多麻煩。

謝謝金金實驗室的大家，從芳馨學姊帶我認識實驗室的日常，教我很多除了分生實驗上的小技巧外還有待人處世上的方法，每次提出不管多大多小的問題，都會從她身上學到有很多不一樣的見解。厲害的黃老師嘉偉兄，從他身上得到了很多動物實驗和社會價值觀上的啟蒙，不管是在 R744 看他磨頭骨時邊看他做實驗邊跟他聊日常，或是到動物中心學怎麼照顧鼠鼠，他都很願意分享他知道的事情，還有謝謝那顆在我遇到人生課題的金莎，突然點醒我還有擁有當下。開始會跟皓元兄講廢話的我，每次看著他做實驗都可以感受到處女座的氣場，不禁很佩服，難怪 data 都很漂亮，而且常常開車載我們去很多地方，實驗室有他跟芳馨學姊、嘉偉跟老師在就像家一樣。平常也很受佳萱的照顧，常常聽她分享一些生活趣事，也從她身上學到很多我沒看過的實驗技巧，還有約翰紅茶飲料團跟好吃到忘記是什麼名字的醬，為實驗生活增添了不少味覺體驗。懂很多的鐠伴學姊也常常幫我們免疫組注意到很多事情，也是個人很好相處的學姊。Dewi is from Indonesia and comes here to study PhD degree. She's just like our mom, and PT always like to call her "Dewi mamaaa" haha. Sometimes when I was in bad mood, you would come and take care of me. It must be a hard choice to come here alone and finish your

PhD degree because you already have a wonderful family. But I think that is because you have a dream and want to make it come true. Hope everything will always be okay on you.

再來是即將要去美國跟加拿大念書的人們。認真很勇敢往前衝的劉臻是我進這間實驗室時心裡的模範，每次看到她很有熱忱的在討論實驗上的東西時心裡總是佩服，稱讚她厲害的時候又都會很謙虛的說這些沒什麼，我心裡都會想怎麼會沒什麼(笑)，希望她可以實現心裡的夢。體貼又有耐心教學弟妹的思妤常常提醒我們很多事情，不管是實驗室的東西或是我們碩班論文該注意的地方，每次都很無私地分享她的東西，還好有她可以依靠，也希望她在國外和更久的將來可以遇到跟她一樣好的人。一年前加入實驗室的艾妮也是邊學新的實驗邊弄行政的東西，還要同時申請國外的研究所，如果心裡沒有很強烈的目標應該會做不到吧，很高興看到她一步步地朝著理想前進(可惜後來沒有機會一起去健身房哈哈哈)，跟她聊天也常讓人覺得她很有想法，希望之後也能去美國跟妳相聚。還有同是助理以後想出國念書每天跟彥霖一起泡咖啡的 Penny，以後就是 centrosome 組的擔當了，加油(笑)。

然後是實驗室同屆的同學們，還好有遇到像你們這麼有趣又有想法的人。不知為何很可以聊內心話的坤銓，相處起來沒有太大的壓力，遇到麻煩時總是不猶豫的說可以幫忙，真的很感謝你，希望不管之後如何都會順利。還有不管到哪都可以開啟網美模式的芃慈也是實驗室好夥伴，好像莫名的就一起接了很多所上跟學校的任務，還好有妳幫大家默默凱瑞了很多事情。冷知識王兼藝術總監及小腦組支柱，名號好長的岳儒每次都會分享很多像是都市傳說的東西(笑)。還有充滿阿玶氣場的玄姊總是可以從他那裡得到很多實驗上的獨到見解，每次都能一針見血的點到很多 BUG。還有很多的話沒能用文字說，但從你們這裡學到了不少，這兩年互相提醒幫助到了畢業，還好實驗室的夥伴是你們。

再來是小碩一們，你們真的是一群很有才華的人。每次都會在 R744 陪我聊天的惠勤雖然有時候會想太多，但體貼的她其實都會比別人想更多，希望妳可以開心的過每一天。宗翰就有點神祕，雖然有點天然呆而且平常看起來很無助(?)，不過其實是個可靠的人，所以宗翰加油，以後免疫組就靠你了(笑)。每天都笑得很開心不過笑點有點奇怪的巧玟，實驗室都會充滿她的笑聲，對很多事情都很有自己的想法，所以常常也會有過不去的時候，以後都會好好的啦不要太擔心(還

有以後中間如果不知道發生什麼事的話，問她就對了)。有很多扭蛋跟療癒小廢物和攝影能力很強的彥霖是工程組的擔當，我們實驗室的 program 就要靠他跟老師了(笑)，感謝他每次都願意跟我講很多廢話，還讓我幫他的扭蛋豬取名叫莫豪。字音字形能力強到可怕的柯醫師皓貞是個很有才很有想法的人，平常看她跟玄姊互相傷害看得駭人…柯醫師加油(笑)。

還有一群年輕有為的大學部學弟妹，總是在課業之餘跑來實驗室做實驗。TED 好夥伴兼充滿學姊氣場的昕儀是個很好相處的女孩(雖然以她的年資真的要叫學姊)，很難得會遇到活動相投的人，不知道為什麼好像跟你認識了很久，感覺你以後不管怎樣都會好好的，希望一切都好:)。聰明優秀的莞茜是個超齡的小孩，內心裡住了一個看透人世間的老人(笑)，不管是實驗或人生規劃上都非常有想法，不愧是莞茜，希望你可以一直這麼優秀。聰穎謙虛的盧謙也是個厲害的學弟，我們一起去花蓮玩的時候受到了他們家不少的照顧，希望你也一切都很好。心思很細膩也可愛的學弟證硯是個有趣的人，常常逗實驗室很多人開心，跟芃慈是一對寶。唯齡也是個會默默出現做實驗很認真的學弟，一直不斷在進步的他將來也會不錯的吧！

當初還有最不能忘的淑惠姊，照顧我們腦科所大小事，有什麼好的機會都會替我們爭取，這一年你好像有些事情沒能來，但我們畢業典禮那天你的突然道來真的就像一道溫暖的陽光灑下來，幫我們整理怎麼穿都不對的碩士袍，關心我們最近過得好不好，也一直笑著跟我們說你很好沒事。還好有你，謝謝你。

最後我想感謝劉祐岑醫師，在妹妹最需要幫助的時候幫了她好多。還有感謝我的家人，謝謝他們容忍我的任性讓我去做我想做的事情，拉拔叛逆的我長大，如果不是他們我也沒辦法順利的完成學業，道不盡的思念及感謝。

「人生不是在等待暴風雨過去，而是要學會在雨中跳舞。」雖然這段日子有很多遺憾，但我知道妳已經自由的在某個地方遨遊。別人都為妳難過，但我替妳感到驕傲，因為妳是個很勇敢又堅強的女孩。

在這條路上得到了很多幫助，還有寫不完的感謝，希望未來的我們都過得很好。

2020/06/16

中文摘要 Chinese Abstract

平腦症為因大腦神經發育異常而造成的疾病，其病理特徵如其名般為平滑的腦，而症狀包含癲癇、運動發展遲緩以及肌肉痙攣等。*DCX* 為在 X 染色體上，所以如果 *DCX* 發生突變，多半遺傳到突變基因的男性都會患有平腦症。Doublecortin 有兩個微管連接區域: N 端區只會和組裝好的微管連結，而 C 端區除了微管也會和未聚合的微管蛋白連結。在與醫師合作下，從六個有平腦症孩童的家庭中找到共通的突變基因 DCX，而這些突變位點都在 C 端微管結合區域。我們的目標是去確認這些突變點是否影響大腦神經發育，並假設因突變 DCX 影響到微管形成和分解，而造成大腦神經發育遷移或細胞分裂異常。為了觀察突變 DCX 在微管形成中是否受影響，利用微管蛋白結合實驗觀察突變 DCX 是否會影響和微管之間連接能力，並利用微管再生實驗讓細胞中微管從去聚合期回到生長期。在微管蛋白結合實驗中，我們看到 p. V177Afs*31、p. G188W、p.K202M 及 p. D262G 會影響結合能力。而微管再生實驗也看到 p. V177Afs*31、p. G188W、p. R196H、p. K202M 及 p. D262G 可能會影響微管生成。對於這個研究，期盼能更加瞭解平腦症的致病機轉以及相關大腦發育異常所導致的疾病。

關鍵字：平腦症、DCX、微管連結蛋白、大腦神經遷移

English Abstract

Lissencephaly is a devastating neurodevelopmental disorder featuring a smooth brain surface and symptoms including seizure, psychomotor retardation, and muscle spasticity. Mutations in *DCX* on the X chromosome were reported to cause the disease in male. *DCX* encodes doublecortin protein, which has two microtubule binding domains: N-terminal domain binds only to assembled microtubules, while the C-terminal domain can bind to microtubules and unpolymerized tubulin. Here we identified DCX mutations, including one truncated and five missense forms, in lissencephaly patients from six families. Most of these mutations are on the C-terminal domain, and our aim is to examine how these mutations affect neuronal development. We hypothesize that DCX mutations may cause defects in microtubule dynamic process during neuronal migration. To confirm the function of DCX mutations in microtubule dynamic process, microtubule binding spin down assay was used to check whether the binding function was altered. Moreover, microtubule regrowth assay was used to test whether these mutations affect microtubule nucleation and/or growth. In microtubule binding assay, we found the binding ability to synthesized taxol-stabilized microtubule was decreased in p. V177Afs*31, p. G188W, p.K202M and p. D262G DCX mutants. Furthermore, in regrowth assay we used U2OS cells expressing these DCX mutants and we found that mutations on p. V177Afs*31, p. G188W, p. R196H, p. K202M and p. D262G caused abnormal microtubule nucleation in cells. This functional study may lead to more understanding of the pathogenic mechanism of lissencephaly and related brain developmental disorders.

Keywords: Lissencephaply, DCX, Microtubule binding protein, Neuronal migration

Contents

List of Figures

List of Supplemental Figures

Chapter 1. Introduction

1-1 Development of the cerebral cortex

During the development of human cerebral cortex, neuronal migration is an essential process that is tightly regulated by varieties of intracellular and extracellular molecules (Buchsbaum and Cappello, 2019). In the early embryonic stages, neural stem cells proliferate by symmetric division in the ventricular zone (VZ) of the developing neural tube to expand their neuroepithelium and radial glia (RG). When neural stem cells undergo symmetric cell mitosis, the nuclei will move to the inner surface of the VZ at G2/M phase to divide into two daughter cells. They then move away from the surface during G1 phase and go through S phase in the subventricular zone (SVZ) before entering into the next cell mitosis. This process is termed interkinetic nuclear migration (Norden et al., 2009; Tsai et al., 2005).

When the layer of neural tube becomes thicker, neurogenesis begin by asymmetric division. RG cells will produce neurons directly or through producing intermediate progenitor (IP) cells and OSVZ radial glial (ORG) cells, which will later divide further to produce more neurons (Buchsbaum and Cappello, 2019; Oksdath et al., 2018). Post-mitotic neuronal precursors will first undergo multipolar migration, and then carry out a multipolar-to-bipolar transition in the SVZ to enter the intermediate zone (IZ). Those neurons then migrate in a bipolar form toward the cortical plate (CP) along radial fibers extended from RG cells. The earliest-born neurons first migrate away and form the pre-layer, the later-born neurons then migrate through the pre-layer and populate on it. Such that the early-born neurons form deeper neocortical layers (layer VI and layer V) and

the later-born neurons develop in superficial layers (layer IV and II/III) and become six layers of cerebral cortex termed into inside-out manner (Greig et al., 2013; Rakic, 1974).

1-2 Somal translocation in neuronal migration of brain development

Newborn neurons have various mechanisms in bipolar-directed migration during developing brain cortex. Two modes of radial migration have been defined in previous studies: locomotion and somal translocation (Nadarajah et al., 2001; Tabata and Nakajima, 2003). The migrating movement is also termed “two stroke model”. In this dynamic leading process, cell microtubules are arranged and point out toward the nucleus from the centrosome. Cytoplasmic dynein concentrates in the swelling area within front edge of migrating neurons, and pull the microtubule network attached to the centrosome from the plus ends to minus ends. The centrosome then will lead the cell body forward.

The cell body can be moved due to the cage-forming microtubules around the nucleus. LIS1-dynein complexes help microtubules attached on the nucleus surface and Doublecortin regulates the microtubules dynamic process, it then becomes a movement in this migration (Tanaka et al., 2004; Tsai et al., 2007).

1-3 Genetic variants in neuronal migration disorders

Development of human cortex is a highly complex process involving a variety of intrinsic and extrinsic mechanism. Thus, if something goes wrong, especially genetic mutations in these fine-tuning neuronal migration, could cause brain neural development disorders, such as lissencephaly (smooth brain), microcephaly (small

brain), macrocephaly (big brain), subcortical band heterotopia (double cortex), periventricular heterotopia, focal cortical dysplasia, attention deficit hyperactivity disorder (ADHD), epilepsy and etc…. Nowadays, genetic evidence pointed out that genetic variants or mutations are the major cause of neural developmental disorders (Buchsbaum and Cappello, 2019; Thapar et al., 2017).

For example, lissencephaly can be caused by mutations in *LIS1*, *DCX*, *ARX*, *RELN*, *TUBA1A* and etc…. (Buchsbaum and Cappello, 2019; Heinzen et al., 2018; Sheen et al., 2006). Mutations on DCX causes X-linked lissencephaly in male and subcortical band heterotopia in female, although some clinical reports also mentioned that they found lissencephaly in female and subcortical band heterotopia in male. *DCX* is located on X chromosome, and because of the X chromosome inactivation, we can see the gender-dependent conditions. (Matsumoto et al., 2001; Zare et al., 2019)

In previous study, it has been demonstrated that some mutations on DCX from subcortical band heterotopia have different defecting level on binding ability by cooperativity assay and turbidity assay. Furthermore, they mentioned that these mutants in clinical study are heterogeneous condition, so those malformation should not be too severe. Moreover, they compared the MRI images with their data, showing the positive correlation between the brain phenotype with their data (Bechstedt and Brouhard, 2012). It's one of the evidences about DCX mosaicism due to X chromosome inactivation in this diverse genetic background.

In our study, all patients have a mutation in *DCX* and are suffered with lissencephaly and subcortical band heterotopia. Lissencephaly is a rare brain disorders, the type I is characterized by smooth brain, nearly loose the gyri and the brain cortex

becomes thicken four-layered cortex (Dobyns and Truwit, 1995). Type II has a common name called cobblestone lissencephaly, known as its appearance brain surface, it is due to neurons over-migrating to cortical surface (Buchsbaum and Cappello, 2019). Children who are with lissencephaly will have the symptoms as follows: psychomotor retardation, failure to grow up, seizures, and muscle spasticity or hypotonia. Nowadays there's no proper therapy for lissencephaly, only some of the symptoms can be controlled well.

1-4 Doublecortin (DCX) and its microtubule binding domain

Doublecortin (DCX) is located on X chromosome. It is a microtubule binding protein, and has two microtubule binding domain. Studies show that N-terminal domain on DCX binds only to assembly microtubules, and the C-terminal domain can bind to microtubules and unpolymerized tubulin (Kim et al., 2003). In previous study, they found the sequence of N-terminal and C-terminal domain has similarities in coding protein sequence through alignment, and that means a similarity three-dimensional fold it has (even though C-terminal domain has variety sequence in the end tail) (Fig. S2) (Kim et al., 2003; Sapir et al., 2000). These two domain are also highly conserved in other species such as C. elegans zyg-8, drosophila melanogaster.

The expression of DCX begins during neural stem cells undergo cell dividing and migrating, those post-mitotic and migrating neurons are regulated by DCX through organizing microtubules dynamic process. Moreover, DCX is important not only in the central nervous system but also peripheral nervous system during embryonic and postnatal development (Gleeson et al., 1999). Thus, if DCX has a mutation, then it's possible to affect neuronal development and cause neuronal migrating disorders.

1-5 The relationship between microtubule and DCX

Microtubules support many types of cellular morphogenesis and migration processes during brain development. It is essential for neurite formation, outgrowth, migration, cargo transport, synapse generation, signaling, and cell division (Aiken et al., 2019; Manka and Moores, 2018). The structure of microtubule is formed by assembling α- and β-tubulin heterodimer. The β-tubulin of heterodimer binds with GTP, and then heterodimers start to arrange together by head-to-tail and side-by-side forming 13-protofilaments (PF). There are four steps followed by after α- and β-tubulin heterodimer activated: (i) nucleation (ii) growth (iii) stabilization (iv) catastrophe, it is called microtubule dynamic, which is driven by GTPase cycle (Manka and Moores, 2018). DCX, a microtubule binding protein, participating in this dynamic by combining four tubulins and organizing the growing of microtubules.

1-6 The variants and mutations on DCX

A schematic diagram of DCX mutants shows the reported mutations (Figure 2A). Most of the mutations has been reported that are found from lissencephaly, subcortical band heterotopia or epilepsy. The mutants we are studying now are all affecting on C-terminal microtubule binding domain, and those are on DCX p.V177Afs*31 (del 11 cDNA), p. G188W (c. G562T), p. R196H (c. G587A), p. K202M (c. A785G), p. T203A (c. A607G) and p. D262G (c. A785G). The pedigree shows DCX p. G188W and p. K202M are familial genetic inheritance, DCX p. R196H is *de novo* mutation (Figure 1). The mutation on V177, G188 and K202 are novel mutation sites, and D262 is our previous study (Tsai et al., 2016).

1-7 Significance

This functional study may lead to more understanding of the pathogenic mechanism of lissencephaly and related brain developmental disorders. We hope this study can help patients and their family get a better therapy.

Chapter 2. Material and Methods

2-1 The approval and registration from clinical patients was in standard procedure

The data of lissencephaly patients were approved by Chia-Yi Christian Hospital, Changhua Christian Hospital, and Chang Gung Memorial Hospital.

2-2 DNA Sanger sequencing

The mutation site of DCX in lissencephaly patients were all confirmed by whole exome sequencing. Sanger sequencing was used to confirm the mutation site through PCR analysis, and the primers were (1) DCX p. G188W (c.562 G>T) Forward primer: 5'-TTCTA CTCCA GTGTC AGTGT G-3', Reverse primer: 5'-TGATT CATTG CTTTG CCTGC-3' ;(2) DCX p.R196H (c.587 G>A) Forward primer: 5'-GTTCT ACTCC AGTGT CAGTG TG-3', Reverse primer: 5'-ATGAG ATGTG GAGGA AGAGT C-3'.

2-3 Plasmids and Mutagenesis construct

EGFP-DCX (Catalog #32852, Addgene) and GST-DCX were prepared in previous study(Tsai et al., 2016). The studies were based on Homo sapiens doublecortin (DCX), transcript variant 2 (NM_178152.3).

To study whether mutated DCX affects brain neuronal development, we used

QuikChange Lightning Site-Directed Mutagenesis Kit (Catalog # 210519, Agilent Technologies) to produce our mutants. EGFP-DCX or GST-DCX was used as wild type template, and the primers were designed as follows:

Mutants	Mutagenesis primer designed
DCX V177A fs*31 (del: 11 codons)	F': 5'-CCAGGGAGAACAAGGACTTTG CTGGTTACCATCATCCGCAGT-3'
	R': 5'-ACTGCGGATGATGGTAACCAG CAAAGTCCTTGTTCTCCCTGG-3'
DCX p.G188W (c.562 G>T)	F': 5'-GTTACCATCATCCGCAGTTGGGTGAAGCCTCGGAAGG-3'
	R': 5'-CCTTCCGAGGCTTCACCCAACTGCGGATGATGGTAAC-3'
DCX p.R196H (c.587 G>A)	F': 5'-AGCCTCGGAAGGCTGTGCATGTGCTTCTGAACAAGAA-3'
	R': 5'-TTCTTGTTCAGAAGCACATGCACAGCCTTCCGAGGCT-3'
DCX p. K202M (c.848 A>T)	F': 5'-GTGTGCTTCTGAACAAGATGACAGCCCACTCTTTTGA-3'
	R': 5'-TCAAAAGAGTGGGCTGTCATCTTGTTCAGAAGCACAC-3'
DCX p.T203A (c.607A>G)	F': 5'-GTGCTTCTGAACAAGAAGGCAGCCCACTCTTTTGAGC-3'
	R': 5'-GCTCAAAAGAGTGGGCTGCCTTCTTGTTCAGAAGCAC-3'
DCX D262G (c.785A > G)	Prepared in previous study.(Tsai et al., 2016)

Finally, the mutated DNA were amplified by PCR, we added DpnI enzyme to select the mutants, then transform DpnI-treated DNA into XL10-Gold Ultracomplement cells to produce our construct. Constructs were amplified in E.coli which were cultured in LB broth, and purify by TOOLS Plasmid Mini Kit (TOOLS, Cat.# TT-A03-3). The sequences of constructs were confirmed by Genomics in Taiwan.

2-4 Cell culture

U2OS cells were maintained in Dulbecco's Modified Eagle Medium PH 7.1~7.2 (gibco, Cat.# 12100-046) with 1.5 g sodium bicarbonate, 0.11 g sodium pyruvate, L-glutamin (1:100), Penicillin/Streptomycin (1:100) and 5% Fetal Bovine Serum. Cells were incubated in 37℃ with 5% CO_2.

2-5 Cell transfection

To observe the binding functions of DCX mutants in microtubules, 6×10^4 U2OS cells were plated on glass cover slip which is coated by poly-D-lysine in each 4-well plate. 0.3 μg EGFP-DCX wildtype or mutants were transfected by Lipofectamine™ 3000 (Invitrogen™) with opti-MEM (Gibco, Catalog # 31985070) in serum-free DMEM medium. Exchanged medium with serum contained DMEM medium after 8 hours. The total transfection time is 24 hour.

2-6 Protein purification

Glutathione Sepharose™ 4B (GE healthcare, Piscataway, USA) was used to purify GST-tagged DCX protein. First, we transformed GST-DCX wildtype, GST-DCX V177Afs*31, GST-DCX p. G188W, GST-DCX p. R196H, GST-DCX p. K202M, GST-DCX T203A and GST-DCX p. D262G plasmids into E. coli strain BL21. Colonies were incubated in LB broth medium with 0.1% ampicillin, 37℃ for 14~16 hours with shaking at 225 rpm. Then the cultured broth was diluted into 1:50, introduced into 50 ml LB broth with 0.1% ampicillin. Until OD_{600} was measured more than 0.4, 0.4 mM IPTG was introduced into cultured broth to induce protein for 3 hours.

To confirm the IPTG-induced protein, the cultured broth was collected in 1 mL at time point 0, 1, 2, 3 hours, and centrifuged it to harvest the pellet, then lysed the bacteria with B-PER reagent (Thermo Scientific). The main lysates were incubated with GST-tagged beads (Glutathione Sepharose™ 4B) at 4℃ for 1 hour. Then GST-tagged beads bounded with protein were centrifuged and washed, stored at -80 ℃.

For doing microtubule spin down assay, GST-tagged beads then eluted by GST-elution buffer (10 mM L-Glutathione reduced, 50 mM Tris-HCl PH8, 10% protease inhibitor and 10% phostop). First, add 100 μl GST-elution buffer into 100 μl resin (beads with PBS), and then rotated it in room temperature at time point 5, 10 and 15 minutes. Each time-pointed samples were all centrifuged at 1000 g for 5 minutes, and transfer the supernatant to clean tubes (To make sure no beads left in tubes, centrifuged 1000 g for 3 minutes and collect supernatant again). And add 5 mM DTT (final concentration) to stabilize protein. Take 10 μl samples to run SDS-page to make sure the protein quality, and tested protein concentration by BCA kit.

2-7 Microtubule spin down assay

Taxol-stabilized microtubule was synthesized by Microtubule Binding Protein Spin-Down Assay Biochem Kit (Cytoskeleton, BK029). For assembling microtubule, first aliquot 200 µl General Tubulin buffer to tube and placed it at 35℃ for 20 minutes. At the same time, defrosted 20 µl Tubulin protein (5 mg/mL) in room temperature water bath, after it thawed transferring it on ice immediately and added 2 µl Cushion buffer, then incubated it at 35℃ for 20 minutes exactly. After incubating General Tubulin buffer in 35℃ water bath for 20 minutes , added 2 µl of 2 mM Taxol stock

solution and mixed well. When finishing the incubated Tubulin protein, took it out immediately and then gently mixed with 200 μl of General Tubulin buffer with Taxol, we can store it at room temperature for few hours. Taxol-stabilized microtubule was already synthesized, it's about 5×10^{11} MT/mL (This is equivalent to 5 μM tubulin dimer or 0.4 nM microtubules).

For testing the binding ability with DCX and microtubule, prepared 300 μl General Tubulin buffer with 3 μl Taxol stock solution and mixed well. Set up the microtubule spin-down assay table below:

Table 1: Positive and negative control:

Tube	Protein	Microtubule (μL)	General Tubulin buffer plus Taxol (μL)
1	MAP2 fraction (16 μl)	20	24
2	BSA (1.5 μl)	20	38.5
3	DCX (300 μg)	20	10
4	DCX (300 μg)	0	30

Table 2: For testing the binding ability of DCX with microtubule:

Tube	Protein (250 μg)	Microtubule (μL)	General Tubulin buffer plus Taxol (μL)
1	DCX WT (15.3 μg/μL), 16.3 μL	10	8.7
2	DCX WT (15.3 μg/μL), 16.3 μL	-	18.7
3	DCX V177A fs*31 (13.5 μg/μL), 18.5 μL	10	6.5
4	DCX V177A fs*31 (13.5 μg/μL), 18.5 μL	-	16.5
5	DCX G188W (14.1 μg/μL), 17.7 μL	10	7.3
6	DCX G188W (14.1 μg/μL), 17.7 μL	-	17.3
7	DCX WT (15.3 μg/μL), 16.3 μL	10	8.7
8	DCX WT (15.3 μg/μL), 16.3 μL	-	18.7
9	DCX R196H (13.8 μg/μL), 18.1 μL	10	6.9
10	DCX R196H (13.8 μg/μL), 18.1 μL	-	16.9

11	DCX K202M (13.9 μg/μL), 18 μL	10	7
12	DCX K202M (13.9 μg/μL), 18 μL	-	17
13	DCX WT (15.3 μg/μL), 16.3 μL	10	8.7
14	DCX WT (15.3 μg/μL), 16.3 μL	-	18.7
15	DCX T203A (12.2 μg/μL), 20.5 μL	10	4.5
16	DCX T203A (12.2 μg/μL), 20.5 μL	-	14.5
17	DCX D262G (14 μg/μL), 17.9 μL	10	7.1
18	DCX D262G (14 μg/μL), 17.9 μL	-	17.1

※ Due to the limitation of equipment, we made it into three group and each of group had one control DCX WT.

Prepared BRB buffer (80 mM PIPES PH 6.8, 1 mM $MgCl_2$, 1 mM EGTA) and Cushion buffer (40% glycerol, 1mM GTP and 20 μM Taxol in BRB buffer) before setting up the spinning down assay (Wang et al., 2013). After modulating the reactions in Table 2, we incubated the reactions at 30℃ for 30 minutes. Samples would then spin down through 2.7 mL cushion buffer, at 45000 r.p.m., 24℃ for 10 minutes [Beckman Optima L-90K Ultracentrifuge with SW55Ti rotor and centrifuge tubes (Beckman, Cat. #326819)].

Collected the 35 μL supernatant on top of the cushion buffer and the pellet with 25 μL 5x sample dye, and then run the SDS pages. Coomassie blue staining (TOOLS) was used to present the protein expression.

2-8 In vitro GST-pull down assay

To quantify GST-tagged protein concentration, we used 2 mg/ml BSA to make a standard curve and ran the SDS-page with 5 μl protein beads, then dye with TOOLS

Quick Stain Protein Staining Reagent (Bio Tools). Image J was used to quantify protein concentration.

E18 / P8 mouse brain cortex (ICR mice) were lysed in RIPA buffer (150 mM NaCl, 1.0% IGEPAL® CA-630, 0.5% sodium deoxycholate, 0.1% SDS, 50 mM Tris, pH 8.0, Sigma-Aldrich), and protein concentration was quantified with BCA protein assay kit (Thermo Fisher). 400 μg brain lysate were incubated with 10 μg GST-DCX or mutants at 4 ℃ overnight. Samples were centrifuged at 10,000 rpm for 5 min at 4 ℃, and washed with GST-binding buffer. PBS was used to suspend and then ran the SDS-page. Immunoblot was performed with mouse monoclonal anti-alpha tubulin antibody (1:5000, Proteintech).

2-9 Western Blotting

For analysis protein expression, 10% SDS page will be used to run the samples then transfer the proteins onto the PVDF membrane (Millipore, Germany). Membranes will be incubated in the blocking buffer (5% milk) for 1 hour, then primary antibodies will be dissolved in blocking buffer overnight at 4 ˚C. Washed with TTBS buffer (0.1 % Tween-20 in TBS buffer), then incubate with secondary antibodies Goat-anti-mouse antibody for 2 hours. ECL reagent (Millipore) will be used to and detected by Luminescence Imaging system LAS-4000 (GE).

2-10 Microtubule regrowth assay

U2OS cell was transfected with EGFP-DCX wildtype or mutants, plated on the cover slip after coating with poly-D-lysine. After cell had been transfected for 24 hour,

removed the cells from incubator and put into 4°C refrigerator with ice for 1 hour. Cell were incubated in the water bath at 37°C for 1, 5 and 10 minutes. The cells would did immunocytochemistry immediately.

2-11 Immunofluorescence staining

The cells were fixed with 3.7% paraformaldehyde, 0.05% glutaraldehyde and 0.5% Triton X-100 in PHEMO buffer (68 mM PIPES, 25 mM HEPES, 15 mM EGTA PH 6.9, 3 mM $MgCl_2$, 10% DMSO), washed with PBS and followed by 50 mM NH_4Cl in PBS. Then blocked the cells with blocking buffer (5% BSA and 5% NGS in PBS) for 1 hour, and incubated with mouse monoclonal anti-alpha tubulin antibody (1:500, Proteintech) at 4°C overnight. Washed with PBS and incubated with secondary antibodies Anti-mouse Alexa Flour 546 antibody (1:500) for 2 hours. For nucleus staining, DAPI/PBS (1:1000) were incubated in 15 minutes. Images were recorded by microscopy.

2-12 Image analysis

All the images were scanned by confocal microscopy (Zeiss LSM 700) for microtubule regrowth assay. Image J software (NIH) was used to analyze the quantification of protein level on microtubule binding assay. For measuring the number and length of centrosomal microtubules, we used Matlab program which was designed by Dr. Tsai. Sholl analysis was first used to center the centrosome site, and the program would set concentric circle stepping by 3 μm away from centrosome. Calculating the number of microtubules (> 3 μm) in each group. We used Zeiss colocalization analysis to see the colocalized coefficient on DCX with tubulins (Zinchuk et al., 2007).

2-13 Statistical analysis

GraphPad Prism software 8 and Microsoft office 2016 Excel were used to perform the analysis of data. One-way ANOVA was used to analyze the data of microtubule binding and regrowth assay, comparing the difference between multiple experimental groups with control ($n \geq 3$, p value < 0.05). Means $\pm$ S.D. and p value were shown on the statistic graph. Kruskal-Wallis test (nonparametric test) was used to analyze the Zeiss colocalization analysis ($n \geq 3$, p value < 0.05). Median with interquartile range and p value were shown on the statistic graph.

Chapter 3. Results

3-1 Identified DCX mutations in lissencephaly patients by whole exome sequencing or Sanger sequencing

Previously, we identified 5 families of patients with lissencephaly or subcortical band heterotopia. Using whole exome and target sequencing, mutations in the DCX gene were found. The lissencephaly patients were from Chia-Yi Christian Hospital, Changhua Christian Hospital and Chang Gung Memorial Hospital. First we used whole exome sequencing (WES) to investigate potential mutated gene which may defect brain neuronal development. Among these patients, we found 5 mutations in *DCX* in these lissencephly patients. Among them, DCX p. V177Afs*31, p. G188W and p. K202M (NM_178152.3) were novel and p. R196H, p. T203A and p. D262G was previously reported. We then used Sanger sequencing to verify the variants (Demelas et al., 2001; Matsumoto et al., 2001; Tsai et al., 2016).

In family I, two lissencephaly patients were confirmed that they had genetic mutation on DCX p. G188W (c. G562T) (Fig. 1A). In family II, patient with subcortical band heterotopia had *de novo* mutation on DCX p. R196H (c. G587A). (Fig. 1B) In family III, they have three children and all of them get the genetic mutation on DCX p. K202M (c. A785G), and their mother was a carrier (Fig. 1C). The youngest daughter and son were with subcortical band heterotopia and lissencephaly (MRI image was shown on Fig. 1C). The mother and the elder sister in this family didn't get any symptom. It is due to the maternal germline mosaicism, which means one of their X chromosome had been inactivated. (Matsumoto et al., 2001) Family IV was confirmed in previous study (Tsai et al., 2016), patients with lissencephaly and subcortical band heterotopia were confirmed that genetic mutation on DCX p. D262G (c. A785G)

affected brain neuronal development.

3-2 DCX mutations affect the binding ability to microtubules

Since doublecortin has been shown to be a microtubule binding protein (Gleeson et al., 1999; Horesh et al., 1999), we first tested whether these *DCX* mutations would affect its binding affinity to microtubules by microtubule binding assay. To test the condition, we used microtubule binding protein fraction (MAPF) and bovine serum albumin (BSA) as positive and negative controls, respectively. As expected, MAPF co-precipitated with taxol-stabilized microtubules while only a small fraction of BSA was found in the pellet (Fig. 4A). Meanwhile, most DCX protein could also co-precipitate with microtubules. Note that some doublecortin could also be found in the pellet without microtubule, presumably due to protein aggregation. These proteins were subtracted for quantitative analysis.

We then made GST-tagged DCX constructs for protein expression in *E. coli*. Constructs expressing wild type (WT) doublecortin, and its mutants V177Afs*31, G188W, R196H, K202M, T203A, and D262G were transduced into BL21 competent cells and proteins were purified using Glutathione-conjugated beads. These proteins were then incubated with taxol-stabilized microtubules and centrifuged. Doublecortin bound to the microtubules were then analyzed by SDS-PAGE electrophoresis and Coomassie Blue staining (Fig. 4). When bound to microtubule, DCX protein was readily observed within the pellet (Fig. 4A and 4B). We found that p. V177Afs*31 had a dramatic decrease in microtubule binding affinity (0.066 ± 0.231 folds, $p<0.05$, one-way ANOVA). p. G188W and p. D262G had a significant decrease in microtubule binding compared to control (0.432 ± 0.156 and 0.554 ± 0.094 folds, $p<0.05$, one-way

ANOVA). The binding of p. R196H and p. K202M to microtubules also slightly decreased although did not reach confidence level of 95% (one-way ANOVA test).

3-3 Localization of WT and mutant DCX in cells

To examine whether these DCX mutants could localize to microtubules, we introduced EGFP-DCX wild type or mutants into U2OS cells and examine their intracellular localization (Fig. 5). We found that wild type DCX was able to colocalize with microtubules as previously reported (Gleeson et al., 1999). V177Afs*31 did not colocalize with microtubules and mostly diffused in the cytoplasm and the nucleus. On the other hand, point mutations G188W, R196H, K202M, T203A, and D262G was most colocalized with microtubules with a slightly diffused pattern in the cytosol. However, this did not appear distinguishable to the wild type DCX.

3-4 Expression of DCX mutants delayed microtubule growth

To examine potential effects of DCX mutations in microtubule dynamics, we used microtubule regrowth assay to look at microtubule polymerization in cells. EGFP-DCX wild type or mutants were introduced into U2OS cells. The cells were then treated with 4˚C for 1 hr to depolymerize all microtubules (Fig. 6B and 6C). Cells were resumed back to 37˚C for 1 and 10 minutes before fixation. We then observed microtubules in these cells using fluorescence confocal microscopy.

At 1 minute after cold treatment, we observed apparent microtubule regrowth in cells transfected with wild type DCX (Fig. 6B and 6C). However, in cells transfected with mutant DCX, microtubule regrowth was retarded at different degrees (Fig. 6D),

with fewer and shorter microtubules radiating from the centrosome. Sholl analysis (Yadav et al., 2016) showed fewer intersections between microtubules and the concentric circles of different radii from the centrosome. The number of intersections of microtubules at 3 μm was in the order of WT > p. T203A > p. D262G > p. G188W > p. K202M > p. R196H > p. V177Afs*31. The number of intersections in all mutants except T203A were significantly different from those in WT DCX-expressing cells.

Interestingly, after 10 min of microtubule regrowth, there was slightly difference in the organization of microtubules in cells expressing DCX WT and mutants (Fig. S3). For DCX wild type, the microtubule grew completely and we can see EGFP-DCX signaling almost co-localize with tubulins. However, we observed a slightly more GFP signals for DCX mutants in the cytosol (Fig. S3). To examine the extent of DCX binding to microtubule in these cells, we analyzed the colocalization of EGFP-DCX WT and mutants to microtubules (Figure 7). We found slightly difference in subcellular localization of DCX p. V177Afs*31, p. T203A and p. D262G, and the median of colocalized coefficient and interquartile range are as follows (Figure 7B, n ≥ 3, Kruskal-Wallis test, nonparametric test).

DCX mutations	Median	Interquartile range	P value
WT	0.2040	0.03250-0.43550	-
V177Afs*31	0.0340	0.00200-0.05150	**0.0264**
G188W	0.0620	0.00100-0.30430	0.0850
R196H	0.1435	0.06850-0.23850	0.9012
K202M	0.0410	0.01050-0.23750	0.0918
T203A	0.0190	0.00750-0.17700	**0.0503**
D262G	0.0240	0.00075-0.21650	**0.0222**

In colocalization analysis plot graph (Figure 7A), the x-axis is EGFP-DCX (green) signals and the y-axis is α-tubulin (red) signals. The plot graph had three area, if EGFP-DCX is colocalized with α-tubulin, the plot on graph would appear on the third area (Figure 7A). The white plot which were shown on cells, presenting the colocalized area with EGFP-DCX and α-tubulin. Compared to wild type, DCX V177Afs*31 had a significantly different morphology in plot graph. Plot graph in other mutants seemed smaller and left-shifting than the wild type.

Although DCX p. G188W, p. R196H and p. K202M had no significantly difference in the colocalization analysis, these mutants may also affect microtubule growing slowly (Figure 7B).

Chapter 4: Conclusion

Microtubule binding spin-down assay and regrowth assay have shown that these DCX mutants would defect the growing of microtubules. The function of DCX is quite important because it regulates microtubule dynamic process during neuronal migration.

In microtubule binding spin-down assay, DCX p. V177Afs*31 had a dramatic decrease in microtubule binding affinity (0.066 ± 0.231 folds, $p<0.05$, one-way ANOVA), and p. G188W and p. D262G had a significant decrease in microtubule binding compared to control (0.432 ± 0.156 and 0.554 ± 0.094 folds, $p<0.05$, one-way ANOVA). Moreover, in microtubule regrowth assay, we found that the number of intersections of microtubules at 3 μm was in the order of WT > p. T203A > p. D262G > p. G188W > p. K202M > p. R196H > p. V177Afs*31 at the 1 minute time-point. We can also found that in 10 minute time-point group, DCX p. V177Afs*31, p. T203A and p. D262G also delay the growing of microtubule.

Combined with these two functional assay, we supposed that DCX p. V177A fs*31, p. G188W, p. K202M and p. D262G significantly affect microtubule formation and the process growing (Figure 8). DCX p. V177A fs*31, p. G188W and p. K202M are novel mutations that have not been reported.

Chapter 5: Discussion

In our study, we demonstrated that DCX p.V177Afs*31, p. R196H, p. K202M and p. D262G affect the binding ability on microtubules, causing the growing microtubules abnormally.

We purified protein of GST-DCX wild type or mutants and mixed them with synthesized taxol-stabilized microtubules to confirm whether the binding ability changed. In our data, we showed that DCX p. V177Afs*31, p. G188W and p. D262G have significant changed. DCX p. 196H and p. K202M are also defect moderately. Moreover, in microtubule regrowth assay, we showed that numbers of microtubules in DCX V177Afs*31, p. R196H, p.K202M and p. D262G were less than the wild type (Figure 4B and 4C).

Combined with these two functional assay, we demonstrated that most of the mutants would defect the function, except DCX p.T203A. We also provide some insight about the related functional assay.

5-1 A similar three-dimensional fold in N- and C-terminal domain of doublecortin

In previous study, it has been shown that aligning with N- and C-terminal amino acid domain of doublecortin revealed similarity three-dimensional structure (Kim et al., 2003). DCX R59L in N-terminal domain was mentioned that it might have some relationship with R186C in C-terminal domain which was reported with SBH (Kim et al., 2003). Interestingly, in our study Gly188 in (C-terminal) also has same amino acid

on Gly61 (N-terminal) and highly conserved in different species (Figure 7 and S2). DCX p. R196H (LIS) and p. T203A (SBHX) were reported in previous reports (Demelas et al., 2001; Matsumoto et al., 2001). In protein structure, microtubule associated protein are known to have electrostatic affinity with negative-charge on tubulins, and mutations on R196H and T203A might be changed the distribution charge on DCX protein surface (Kim et al., 2003). Thus, mutations on amino acid might cause electrostatic charge changed and affect the function of DCX binding affinity.

5-2 GST-DCX pull down assay may not suitable to see microtubule binding ability

At the beginning, to see whether DCX mutants affect the functions of interacting with microtubule, we used GST-protein tagged pull down assay, purifying GST-DCX wild type/mutated protein and E18/P8 mouse brain cortex protein and then mixed them overnight at 4°C. We can see DCX p.G188W, p. K202M and p.D262G may interact with tubulin more than wild type (Figure S1A). However, we found that this assay may not present the real condition of DCX binding affinity, due to the following reasons: (i) when collecting the microtubule protein, we used sonicator to take the protein from brain. However, this may destroy the structure of microtubules. (ii) We mixed the protein in 4°C, but microtubules would depolymerized at low temperature.

DCX should participate in the polymeration of microtubules, so we think that the GST-tagged pull down assay might not suitable for observing the binding ability. Thus, we then used another microtubule binding assay (Cytoskeleton, BK029), synthesizing the taxol-stabilized microtubules to confirm whether the mutants would defect the ability or not.

But throwing back to this data, according to previous study (Kim et al., 2003), it has been demonstrated that N-terminal domain would like to bind to assembled microtubules, and the C-terminal domain can bind to not only microtubules but unpolymerized tubulin. Hence, based on this knowledge, we assumed that the reason why the interaction of DCX wild type and brain cortex tubulin is not really well in data because of the depolymerized microtubule (Figure S1A), while some mutants would interact with tubulins more than wild type, may due to the functions of C-terminal domain had been changed, so it bound more unpolymerized tubulins. Moreover, most of our mutants are on C-terminal domain, we aligned the mutation site and found p.G188W is highly conserved in two microtubule binding domain (Kim et al., 2003) and also in different species (Figure 3 and Figure S2), while p. R196H, p. K202M and p. D262G also have highly conserved in different species (Figure 3).

DCX highly expresses in immature brain cortex during brain neurogenesis, so the protein level of DCX in postnatal 8 days (P8) from ICR mouse brain cortex was less than E18 (Figure S1C). Thus, after GST pull down assay, the α-tubulin protein level in P8 seemed similar to DCX with E18 brain cortex that may be due to this reason (Figure S1B).

5-3 Aggregation or denaturation of DCX in microtubule binding assay

In microtubule spin down assay, DCX protein still appeared in pellet without microtubules group. It might due to protein aggregation or denaturation, so that we can see some protein band. Moreover, comparing to wild type, the protein level of DCX mutants in pellet without microtubules seems more than wild type, especially DCX p. G188W, p. R196H and p. D262G. In this issues, before we did the microtubule spin

down assay, 5 mM Dithiothreitol (DTT) was added to stabilize the protein structure, and then centrifuge them for removing the aggregated or denatured protein. Thus, we can exclude the problems and make all conditions on the same line.

The DCX mutations might affect protein structure so that defecting the microtubule binding affinity.

5-4 DCX mutants may affect the speed of growing microtubules

DCX plays an important role in brain neuronal development, when neural progenitors migrate to cortical plate through radial glia cell's fiber, the centrosomal microtubules would package the nucleus like a cage, and then guide the cells to the upper layer (Figure 8). DCX participated in this leading process through modulating the microtubule dynamic process (Figure 5A).

To see whether mutations would affect the formation of microtubules, we first introduced EGFP-DCX wild type or mutants into U2OS cells. However, we didn't see the significant differences with control, except p. V177A fs*31 (Figure 5). We supposed if we want to see the effects in DCX mutants, then we need to consider the microtubule dynamic manner maybe the issue we have to focus on. Thus, we lead the EGFP-DCX-transfected cells entering into depolymerized stage and re-growing it. Finally, we found the differences.

In DCX p. V177Afs*31 group, the microtubule in cells still could grow through other microtubule binding protein, but DCX p. V177Afs*31 couldn't bind with tubulins (Figure 6B). At the same time, in other group we also observe that DCX mutants were

not all co-localize with tubulins, which means those mutants couldn't bind to tubulins properly neither, such as DCX p. G196H and p. K202M that frequently had this phenotype. Furthermore, the average of the microtubule intersection in mutants were also lower than control, which means the speed of growing might be slower because of the microtubule dynamic process defected. Finally, we had confirmed that these mutants affect microtubule growing.

We also observe the exchange between the time point at 10 minutes group and used Zeiss colocalization analysis to calculate whether it has significances or not (Figure 7). Those mutants still have some EGFP-DCX signaling in cytoplasm, it could be said that these mutant lead microtubules growing slower. However, there's no apparent differences between wild type and mutants (Figure 7B).

5-5 Defected microtubules might cause neuronal migration delay or post-mitotic cells damaged.

In our project, we found that most mutations would affect the growing microtubule formation. It might have some affection as follows: (i) During brain neurogenesis, cell neuronal migration might be damaged due to microtubules cannot package nucleus well (Figure 8). (ii) Microtubules are the key to complete the cell mitosis, so in post-mitotic neuron cell during neurogenesis, mutations on DCX also might cause maturing neurons.

Chapter 6. Reference

Aiken, J., Moore, J.K., and Bates, E.A. (2019). TUBA1A mutations identified in lissencephaly patients dominantly disrupt neuronal migration and impair dynein activity. Hum Mol Genet *28*, 1227-1243.

Bechstedt, S., and Brouhard, G.J. (2012). Doublecortin recognizes the 13-protofilament microtubule cooperatively and tracks microtubule ends. Dev Cell *23*, 181-192.

Buchsbaum, I.Y., and Cappello, S. (2019). Neuronal migration in the CNS during development and disease: insights from in vivo and in vitro models. Development *146*.

Demelas, L., Serra, G., Conti, M., Achene, A., Mastropaolo, C., Matsumoto, N., Dudlicek, L.L., Mills, P.L., Dobyns, W.B., Ledbetter, D.H.*, et al.* (2001). Incomplete penetrance with normal MRI in a woman with germline mutation of the DCX gene. Neurology *57*, 327-330.

Dobyns, W.B., and Truwit, C.L. (1995). Lissencephaly and other malformations of cortical development: 1995 update. Neuropediatrics *26*, 132-147.

Gleeson, J.G., Lin, P.T., Flanagan, L.A., and Walsh, C.A. (1999). Doublecortin is a microtubule-associated protein and is expressed widely by migrating neurons. Neuron *23*, 257-271.

Greig, L.C., Woodworth, M.B., Galazo, M.J., Padmanabhan, H., and Macklis, J.D. (2013). Molecular logic of neocortical projection neuron specification, development and diversity. Nat Rev Neurosci *14*, 755-769.

Heinzen, E.L., O'Neill, A.C., Zhu, X., Allen, A.S., Bahlo, M., Chelly, J., Chen, M.H., Dobyns, W.B., Freytag, S., Guerrini, R.*, et al.* (2018). De novo and inherited private variants in MAP1B in periventricular nodular heterotopia. PLoS Genet *14*, e1007281.

Horesh, D., Sapir, T., Francis, F., Wolf, S.G., Caspi, M., Elbaum, M., Chelly, J., and Reiner, O. (1999). Doublecortin, a stabilizer of microtubules. Hum Mol Genet *8*, 1599-1610.

Kim, M.H., Cierpicki, T., Derewenda, U., Krowarsch, D., Feng, Y., Devedjiev, Y., Dauter, Z., Walsh, C.A., Otlewski, J., Bushweller, J.H.*, et al.* (2003). The DCX-domain tandems of doublecortin and doublecortin-like kinase. Nat Struct Biol *10*,

324-333.

Manka, S.W., and Moores, C.A. (2018). The role of tubulin-tubulin lattice contacts in the mechanism of microtubule dynamic instability. Nat Struct Mol Biol *25*, 607-615.

Matsumoto, N., Leventer, R.J., Kuc, J.A., Mewborn, S.K., Dudlicek, L.L., Ramocki, M.B., Pilz, D.T., Mills, P.L., Das, S., Ross, M.E.*, et al.* (2001). Mutation analysis of the DCX gene and genotype/phenotype correlation in subcortical band heterotopia. Eur J Hum Genet *9*, 5-12.

Nadarajah, B., Brunstrom, J.E., Grutzendler, J., Wong, R.O., and Pearlman, A.L. (2001). Two modes of radial migration in early development of the cerebral cortex. Nat Neurosci *4*, 143-150.

Norden, C., Young, S., Link, B.A., and Harris, W.A. (2009). Actomyosin is the main driver of interkinetic nuclear migration in the retina. Cell *138*, 1195-1208.

Oksdath, M., Perrin, S.L., Bardy, C., Hilder, E.F., DeForest, C.A., Arrua, R.D., and Gomez, G.A. (2018). Review: Synthetic scaffolds to control the biochemical, mechanical, and geometrical environment of stem cell-derived brain organoids. APL Bioeng *2*, 041501.

Rakic, P. (1974). Neurons in rhesus monkey visual cortex: systematic relation between time of origin and eventual disposition. Science *183*, 425-427.

Sapir, T., Horesh, D., Caspi, M., Atlas, R., Burgess, H.A., Wolf, S.G., Francis, F., Chelly, J., Elbaum, M., Pietrokovski, S.*, et al.* (2000). Doublecortin mutations cluster in evolutionarily conserved functional domains. Hum Mol Genet *9*, 703-712.

Sheen, V.L., Ferland, R.J., Harney, M., Hill, R.S., Neal, J., Banham, A.H., Brown, P., Chenn, A., Corbo, J., Hecht, J.*, et al.* (2006). Impaired proliferation and migration in human Miller-Dieker neural precursors. Ann Neurol *60*, 137-144.

Tabata, H., and Nakajima, K. (2003). Multipolar migration: the third mode of radial neuronal migration in the developing cerebral cortex. J Neurosci *23*, 9996-10001.

Tanaka, T., Serneo, F.F., Higgins, C., Gambello, M.J., Wynshaw-Boris, A., and Gleeson, J.G. (2004). Lis1 and doublecortin function with dynein to mediate coupling of the nucleus to the centrosome in neuronal migration. J Cell Biol *165*, 709-721.

Thapar, A., Cooper, M., and Rutter, M. (2017). Neurodevelopmental disorders. The Lancet Psychiatry *4*, 339-346.

Tsai, J.W., Bremner, K.H., and Vallee, R.B. (2007). Dual subcellular roles for LIS1

and dynein in radial neuronal migration in live brain tissue. Nat Neurosci *10*, 970-979.

Tsai, J.W., Chen, Y., Kriegstein, A.R., and Vallee, R.B. (2005). LIS1 RNA interference blocks neural stem cell division, morphogenesis, and motility at multiple stages. J Cell Biol *170*, 935-945.

Tsai, M.H., Kuo, P.W., Myers, C.T., Li, S.W., Lin, W.C., Fu, T.Y., Chang, H.Y., Mefford, H.C., Chang, Y.C., and Tsai, J.W. (2016). A novel DCX missense mutation in a family with X-linked lissencephaly and subcortical band heterotopia syndrome inherited from a low-level somatic mosaic mother: Genetic and functional studies. Eur J Paediatr Neurol *20*, 788-794.

Wang, W.J., Tay, H.G., Soni, R., Perumal, G.S., Goll, M.G., Macaluso, F.P., Asara, J.M., Amack, J.D., and Tsou, M.F. (2013). CEP162 is an axoneme-recognition protein promoting ciliary transition zone assembly at the cilia base. Nat Cell Biol *15*, 591-601.

Yadav, P., Selvaraj, B.T., Bender, F.L., Behringer, M., Moradi, M., Sivadasan, R., Dombert, B., Blum, R., Asan, E., Sauer, M.*, et al.* (2016). Neurofilament depletion improves microtubule dynamics via modulation of Stat3/stathmin signaling. Acta Neuropathol *132*, 93-110.

Zare, I., Paul, D., and Moody, S. (2019). Doublecortin Mutation in an Adolescent Male. Child Neurol Open *6*, 2329048X19836589.

Zinchuk, V., Zinchuk, O., and Okada, T. (2007). Quantitative colocalization analysis of multicolor confocal immunofluorescence microscopy images: pushing pixels to explore biological phenomena. Acta Histochem Cytochem *40*, 101-111.

Figure 1.

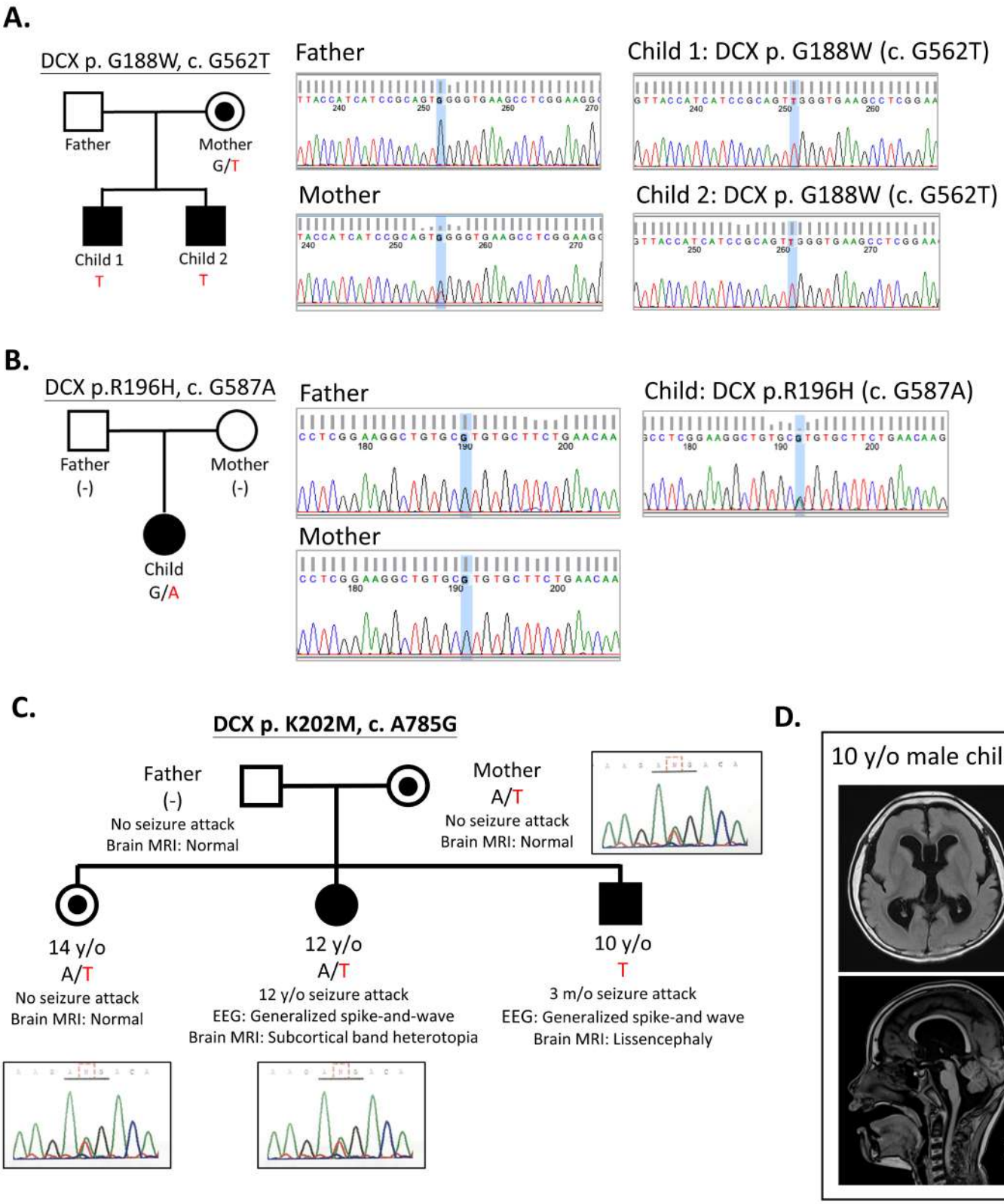
A.
DCX p. G188W, c. G562T
Father
Mother
G/T
Child 1
T
Child 2
T
Father
Child 1: DCX p. G188W (c. G562T)
Mother
Child 2: DCX p. G188W (c. G562T)
B.
DCX p.R196H, c. G587A
Father
(-)
Mother
(-)
Child
G/A
Father
Child: DCX p.R196H (c. G587A)
Mother
C.
DCX p. K202M, c. A785G
Father
(-)
No seizure attack
Brain MRI: Normal
Mother
A/T
No seizure attack
Brain MRI: Normal
14 y/o
A/T
No seizure attack
Brain MRI: Normal
12 y/o
A/T
12 y/o seizure attack
EEG: Generalized spike-and-wave
Brain MRI: Subcortical band heterotopia
10 y/o
T
3 m/o seizure attack
EEG: Generalized spike-and wave
Brain MRI: Lissencephaly
D.
10 y/o male child

Figure 1. Pedigrees and MRI images from the lissencephaly patients.

(A) Patients with lissencephaly carrying genetic mutation on DCX p. G188W (c. G562T), while their mother is a carrier but doesn't have any symptom.

(B) The patient with lissencephaly but her mother is not a carrier, presenting that it's a *de novo* mutation. The mutation is on DCX p. R196H (c. G587A).

(C) A pedigree shows that the missense mutation on DCX p. K202M (c. A785G), and the youngest daughter and son are with subcortical band heterotopia and lissencephaly. While the mother is a carrier, but she doesn't have any symptom. The situation on the elder sister is same as her mother. It's due to the X chromosome inactivation, so that the mother and the elder sister doesn't have any symptoms.

(D) Brain MRI image from the youngest lissencephaly patient with p. K202M in Changhua Christian Hospital.

Figure 2.

A.

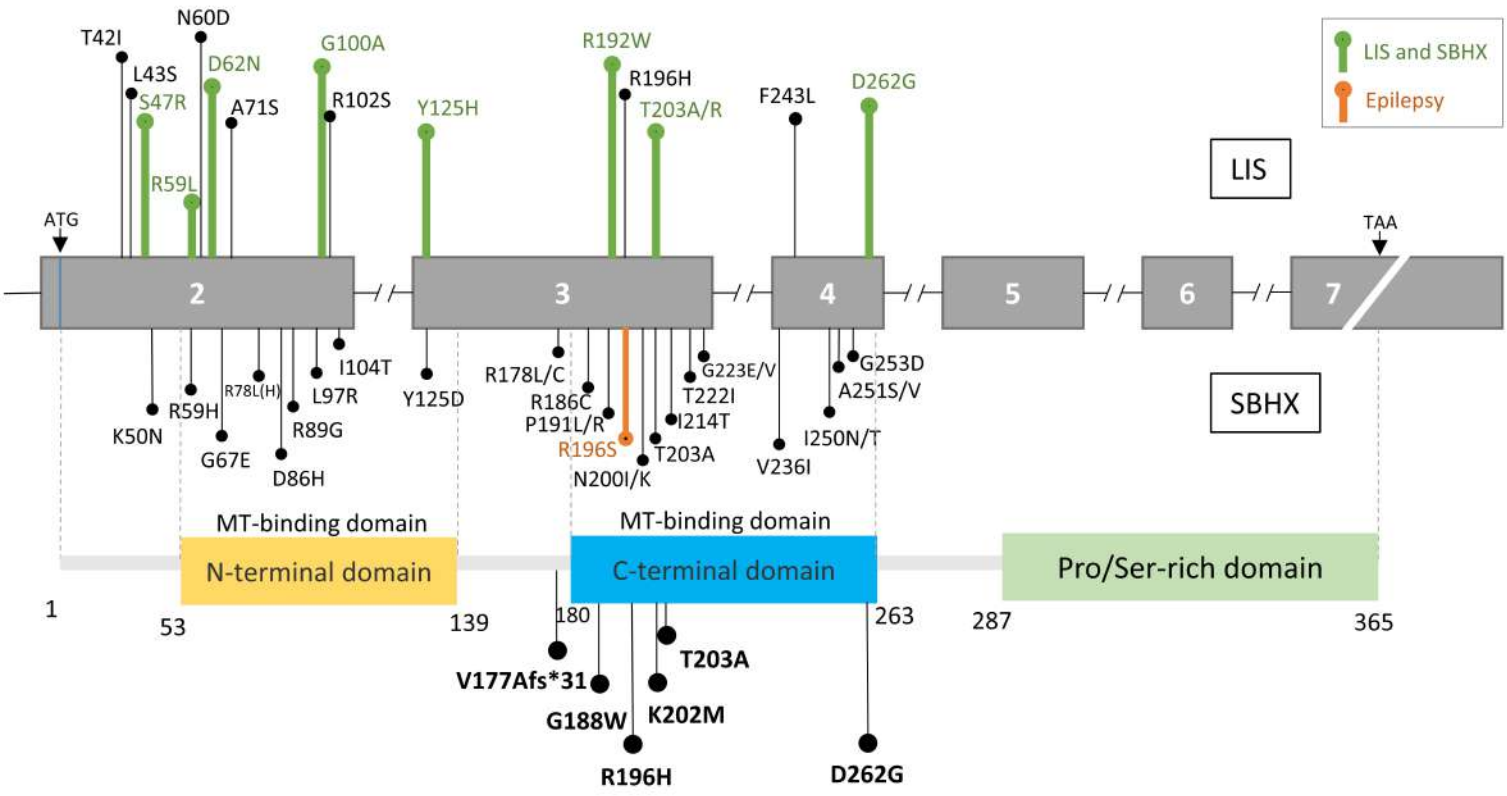

B.

Patient	Amino acid change	cDNA change	Phenotype
1	p. Val177Ala fs*31	del 11 codons	LIS
2	p. Gly188Trp	c. G562T	LIS
3	p. Arg196His	c. G587A	SBH
4	p. Lys202Met	c. A785G	LIS/SBH
5	p. Thr203Ala	c. A607G	LIS
6	p. Asp262Gly	c. A785G	LIS/SBH

Figure 2. The varients on DCX of lissencephaly (LIS) and subcortical band heterotopia X-linked (SBHX) patients.

(A) The exons are shown as gray box. The missense mutation are represented on it. Those mutations which are on the top of exons is clinical reports from lissencephaly and the bottom one are with subcortical band heterotopia X-linked. Missense mutations with green mark have both LIS and SBHX symptom, while with orange mark is with epilepsy (UniProtKB-O43602 DCX_HUMAN; Matsumoto et al., 2001). The protein structure of doublrcortin is shown below the map of exons. Doublecortin has two microtubule binding domain, the N-terminal microtubule binding domain is shown as yellow box, the C-terminal microtubule binding domain is shown as blue box while the Pro/Ser-rich domain is shown as green box. Mutants which we focus on, such as p. G188W, p. R196H, p. K202M, p. T203A and p. D262G are on the C-terminal microtubule binding domain. Frameshift mutant on p.V177Afs*31 also truncate the C-terminal microtubule binding domain.

(B) Table shows the mutations on DCX from our lissencephaly and subcortical band heterotopia X-linked patients.

Figure 3.

Figure 3. Alignment of *DCX* in different species.

Yellow and blue box shows the N- and C-terminal microtubule binding domain, and the missense and frameshift mutation sites are highlighted with 6 different colors. The species includes *Homo sapiens (Human)* (O43602), *Pan troglodytes (Chimpanzee)* (H2R3N6), *Macaca nemestrina (Pig-tailed macaque)* (A0A2K6BJB6), *Rattus norvegicus (Rat)* (Q9ESI7), *Mus musculus (Mouse)* (O88809), *Gallus gallus* (Chicken) (Q98SS5), *Caenorhabditis elegans* (Q95QC4). All amino sequences and alignment are from Uniprot. com. * repsents highly conserved in species.

Figure 4.

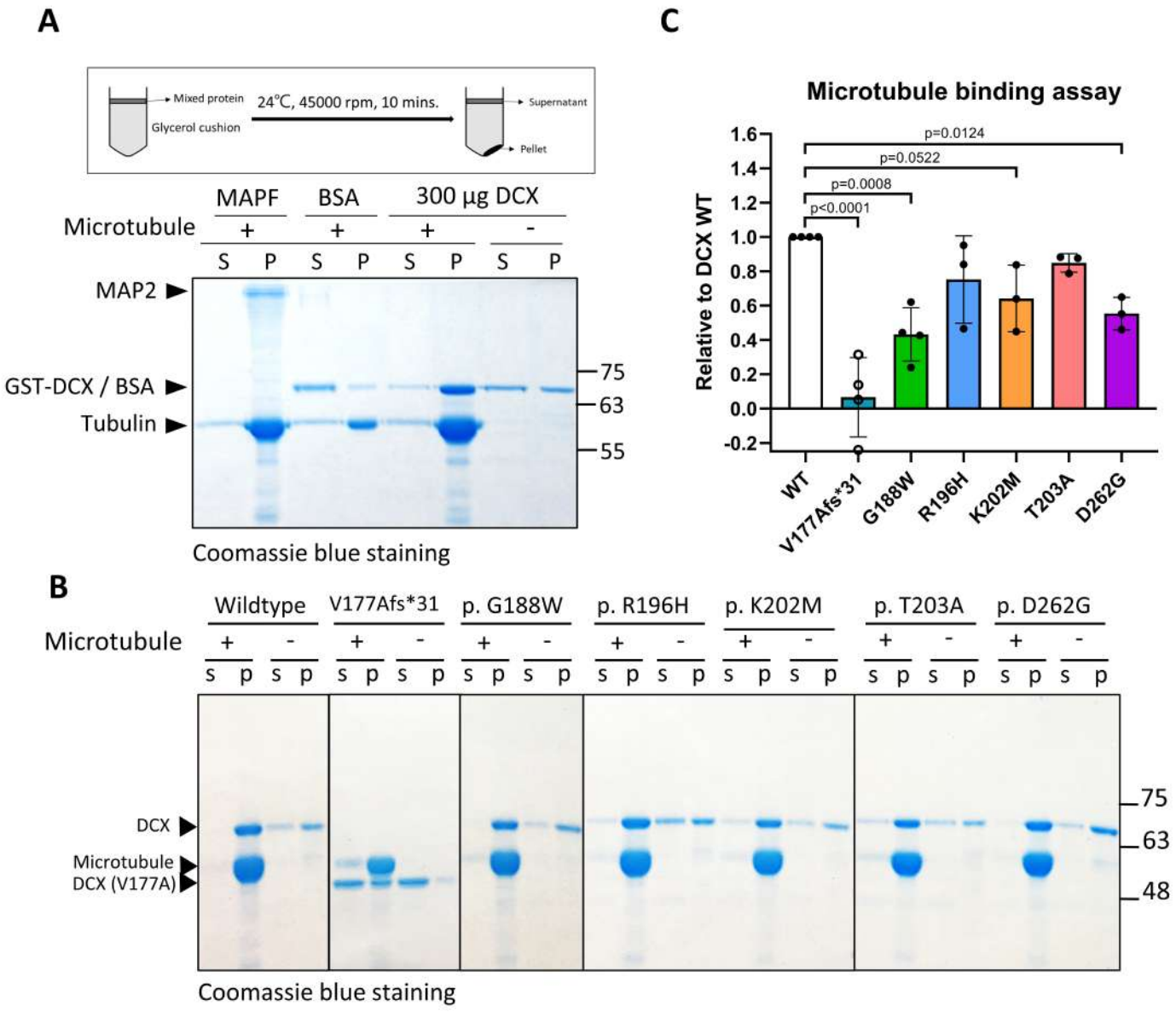

Figure 4. DCX mutations affect the binding ability to microtubule.

(A) Purified 1 mg/mL microtubule associated protein fraction (MAPF), 5 mg/mL bovine serum albumin (BSA) and 300 μg DCX protein mixed with synthesized taxol-stabilized microtubule and then used high-speed centrifuge to spin down it. As a positive control with MAPF and negative control with BSA, it showed MAPF band in pellet and BSA band in supernatant. Purified DCX bound with taxol-stabilized microtubule and showed the band in pellet. S is supernatant and P is pellet. Coomassie blue staining was used to represent the data.

(B) Purified DCX protein 250μg mixed with synthesized taxol-stabilized microtubule, incubating at 30˚C for 20 minutes and then used high-speed centrifuge to spin down it. For quantifying the protein, the protein level of DCX with microtubule in pellet first minus the DCX without microtubule in pellet, then standardized with protein level of microtubule.

(C) DCX p. V177Afs*31 had a dramatic decrease in microtubule binding affinity (0.066 ± 0.231 folds, $p<0.05$, one-way ANOVA). p. G188W and p. D262G had a significant decrease in microtubule binding compared to control (0.432 ± 0.156 and 0.554 ± 0.094 folds, $p<0.05$, one-way ANOVA). The binding of p. R196H and p. K202M to microtubules also slightly decreased although did not reach confidence level of 95% ($n \geq 3$, one-way ANOVA test).

Figure 5.

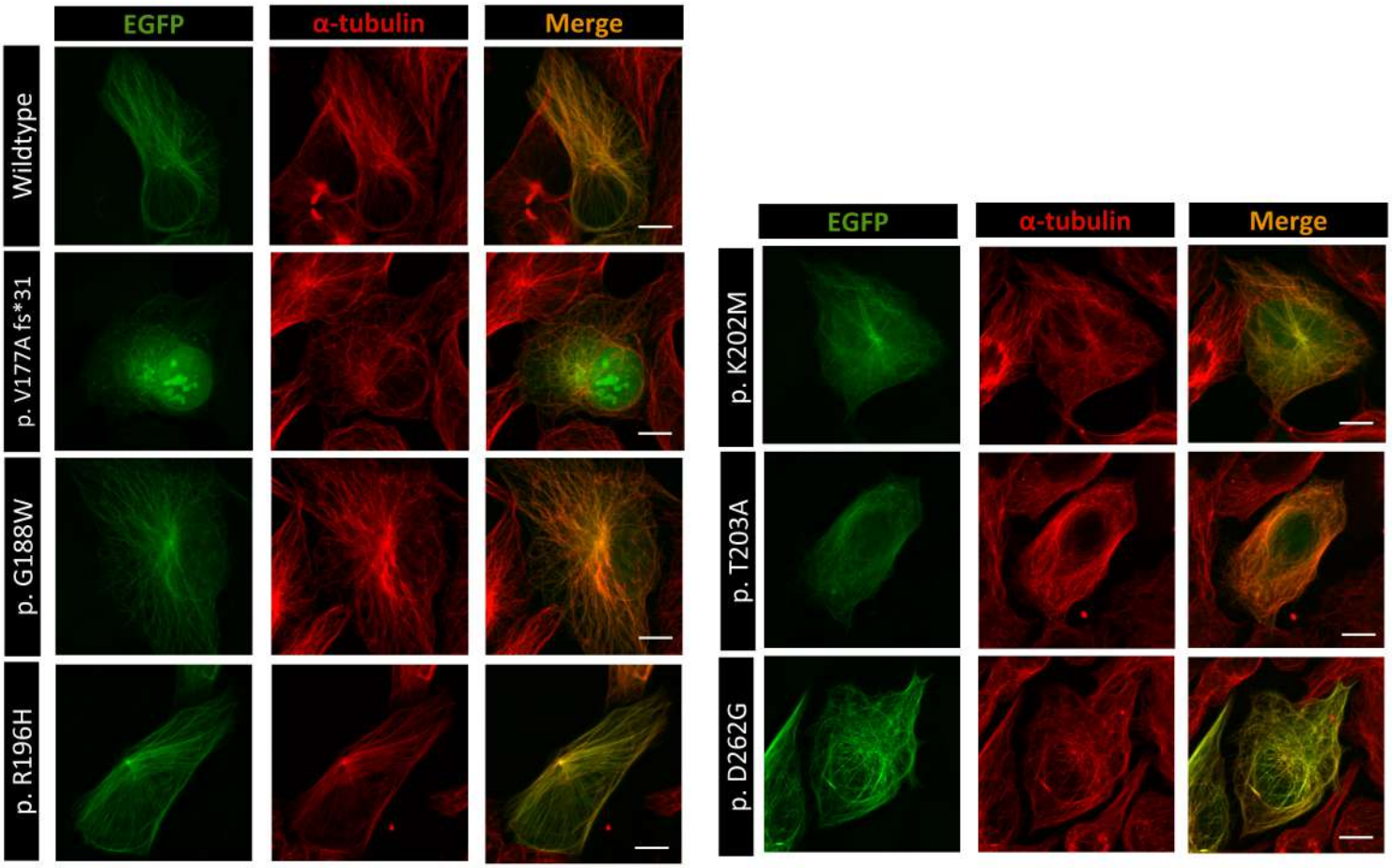

Figure 5. Transfected EGFP-DCX wildtype or mutants in U2OS cell.

We introduced EGFP-DCX wild type or mutants into U2OS cells; however, the cell morphology seemed not apparently different except p. V177A fs*31. The cytoskeletal structure in DCX p. V177Afs*31 group seemed to be destroyed, and the frameshift DCX protein would like to gather in nucleus. Green signal is EGFP-DCX, red signal is α-tubulin and yellow signal is that EGFP-DCX was colocalized with α-tubulin. Scale bar: 10 μm.

Figure 6.

A.

The time point of Re-Growth stage:

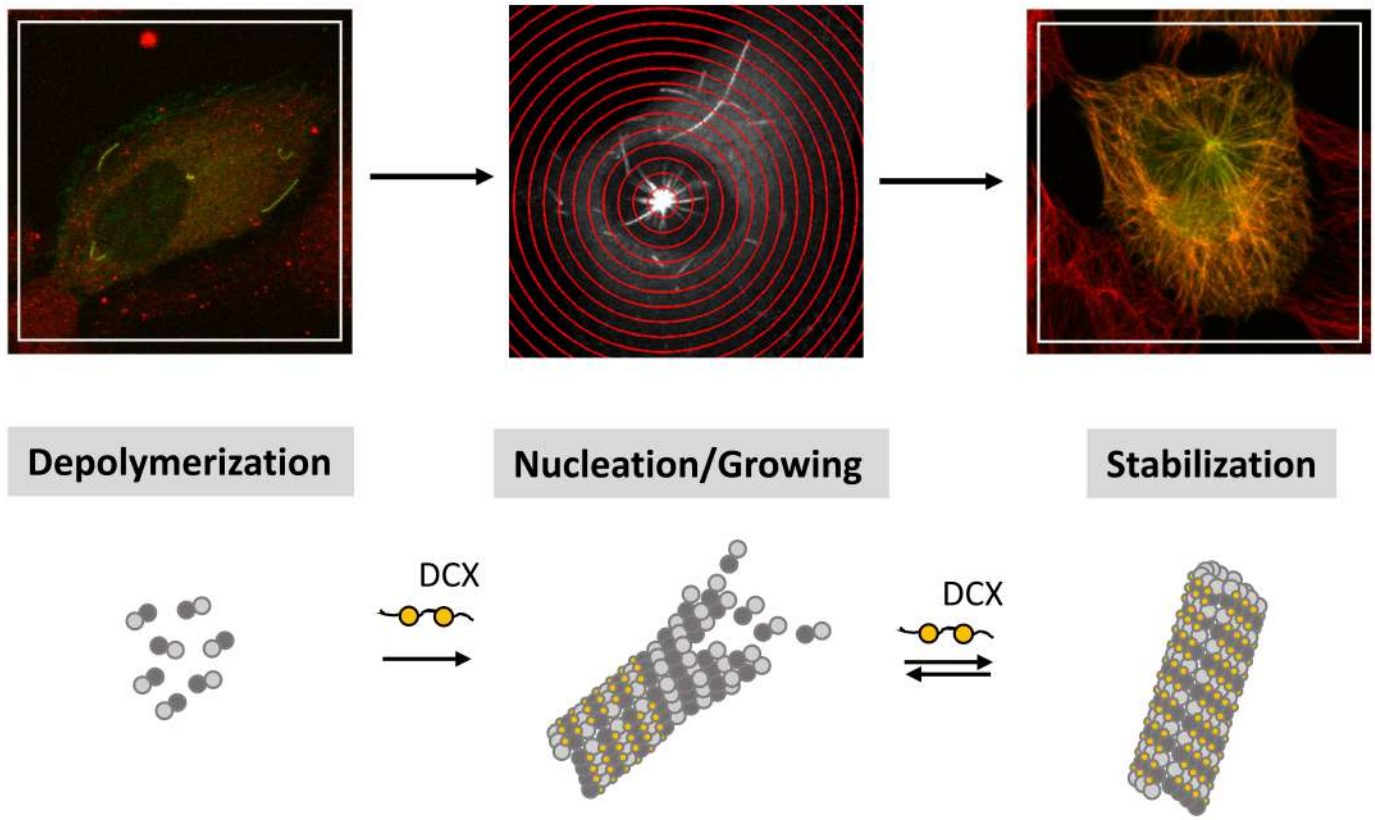

Figure 6.

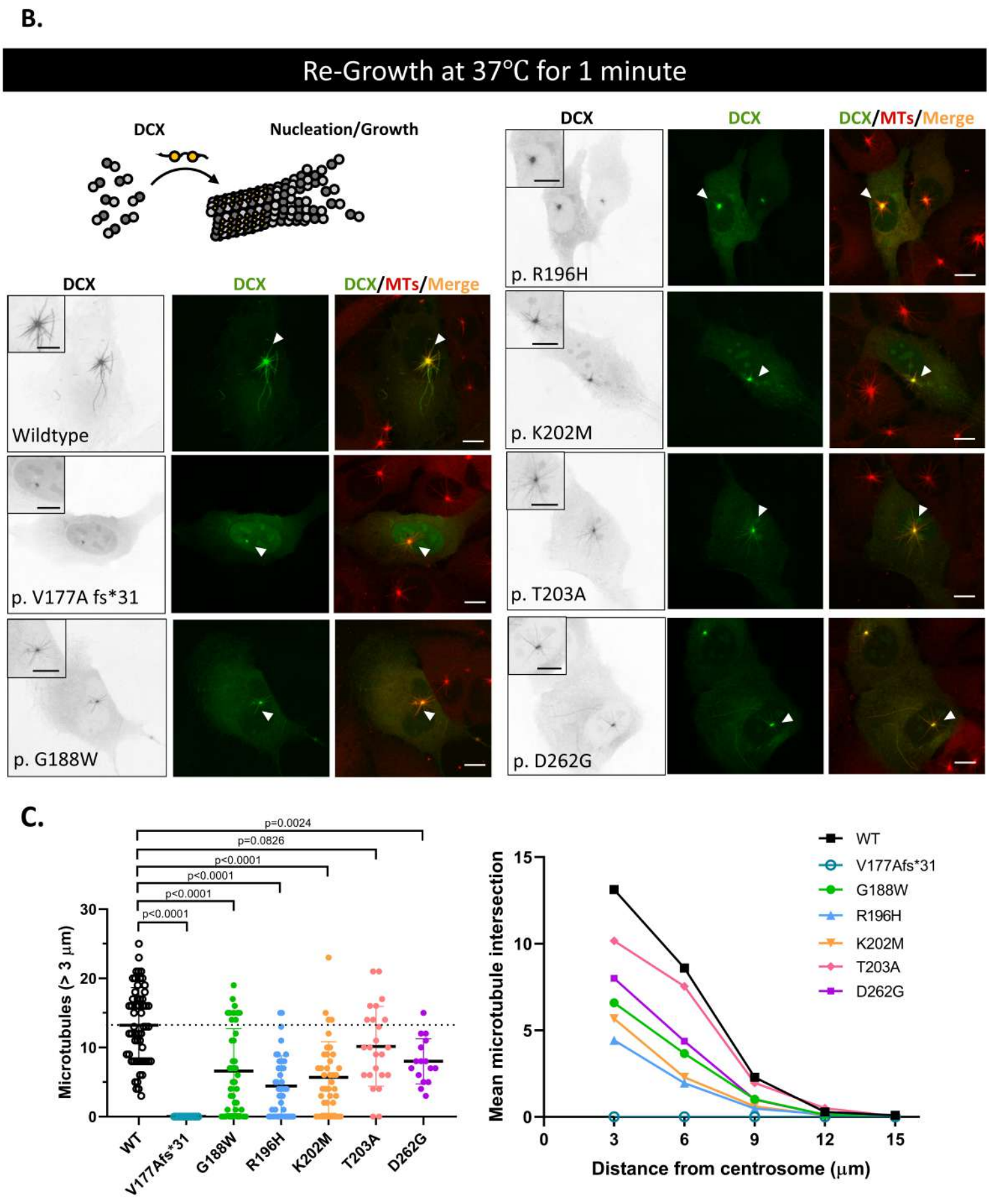
B.
Re-Growth at 37°C for 1 minute
DCX
Nucleation/Growth
DCX
DCX
DCX/MTs/Merge
Wildtype
p. V177A fs*31
p. G188W
p. R196H
p. K202M
p. T203A
p. D262G
C.
p=0.0024
p=0.0826
p<0.0001
p<0.0001
p<0.0001
p<0.0001
Microtubules (> 3 μm)
WT
V177Afs*31
G188W
R196H
K202M
T203A
D262G
Mean microtubule intersection
Distance from centrosome (μm)
WT
V177Afs*31
G188W
R196H
K202M
T203A
D262G

Figure 6. DCX mutations caused microtubule growing slowly in the growth stage.

(A) Microtubule regrowth assay was used to see the relationship with DCX mutants and growing microtubule. EGFP-DCX WT or mutants were transfected in U2OS cells. Cold treating to lead microtubule entering into depolymerization stage and then recovered it at 37℃ for 1 and 10 minute. We used sholl analysis to quantify the intersection by 3 μm concentric circles. While microtubule dynamic process has four steps: nucleation, growing, stabilization and depolymerization. DCX binds four tubulins and help to growing the microtubules. (Manka and Moores, 2018)

(B) Re-growth the cells at 37℃ for 1 minute. DCX p. V177Afs*31 could not bind on microtubules properly, the microtubules in p.G188W and p. R196H were also less than the wild type. Microtubules in DCX p. K202M and p. D262G had significantly less than wild type. Scale bar: 10 μm.

(C) Quantification of the number and the mean of microtubules intersection (length > 3 μm). DCX p. V177Afs*31, p. R196H, p. K202M and p. D262G had significant differences compared to wild type ($p<0.005$), while DCX p. T203A had slightly different ($p=0.0826$). Analysis of the speed of growing microtubules, DCX p. V177Afs*31 had a dramatic difference compared to wild type. DCX p. R196H, p. K202M and p. D262G were also had significantly changed, except the p. T203A. ($n \geq 3$, $p<0.05$, one-way ANOVA)

Figure 7.

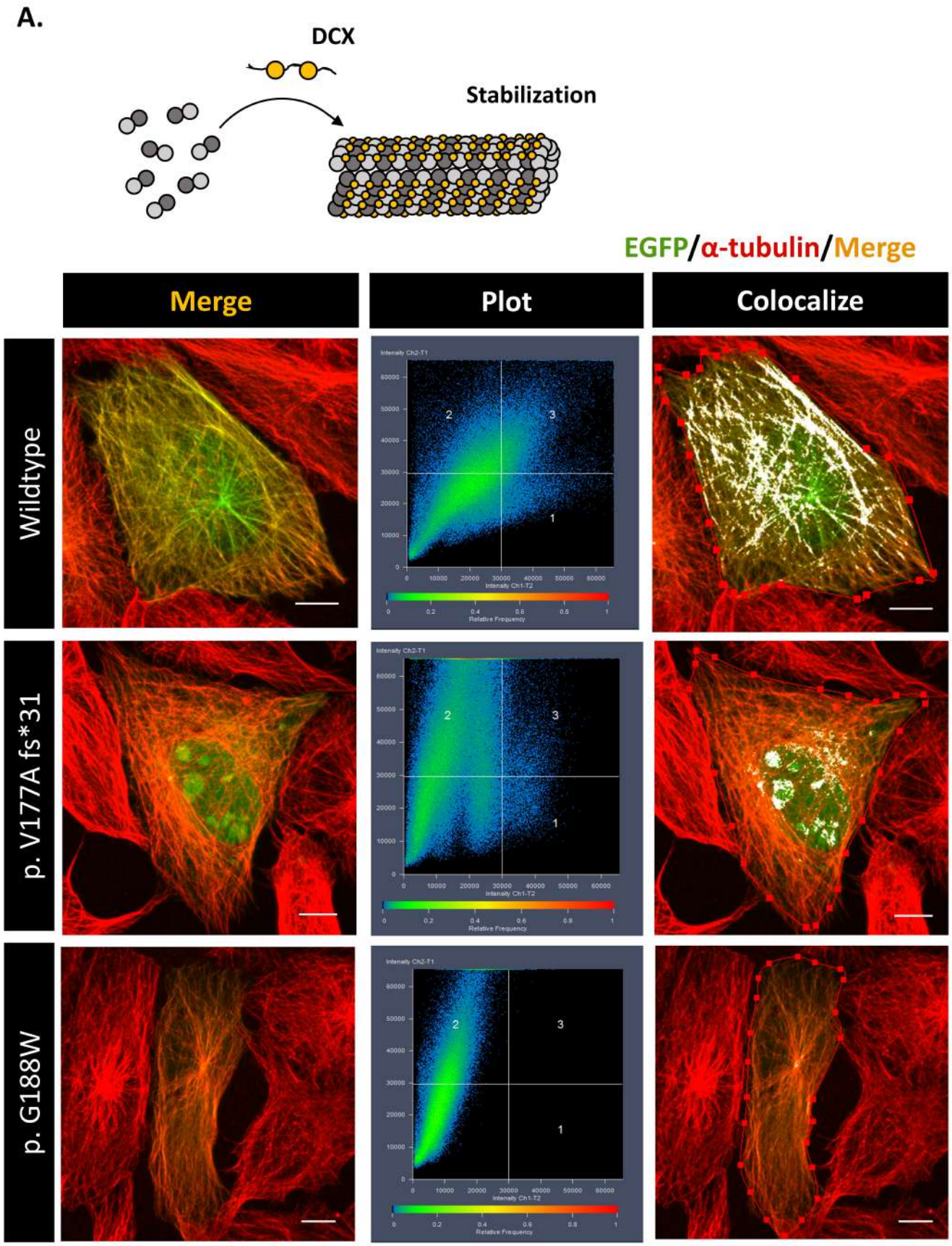
A.
DCX
Stabilization
EGFP/α-tubulin/Merge
Merge
Plot
Colocalize
Wildtype
p. V177A fs*31
p. G188W
Intensity Ch2-T1
Intensity Ch1-T2
Relative Frequency
1
2
3

Figure 7.

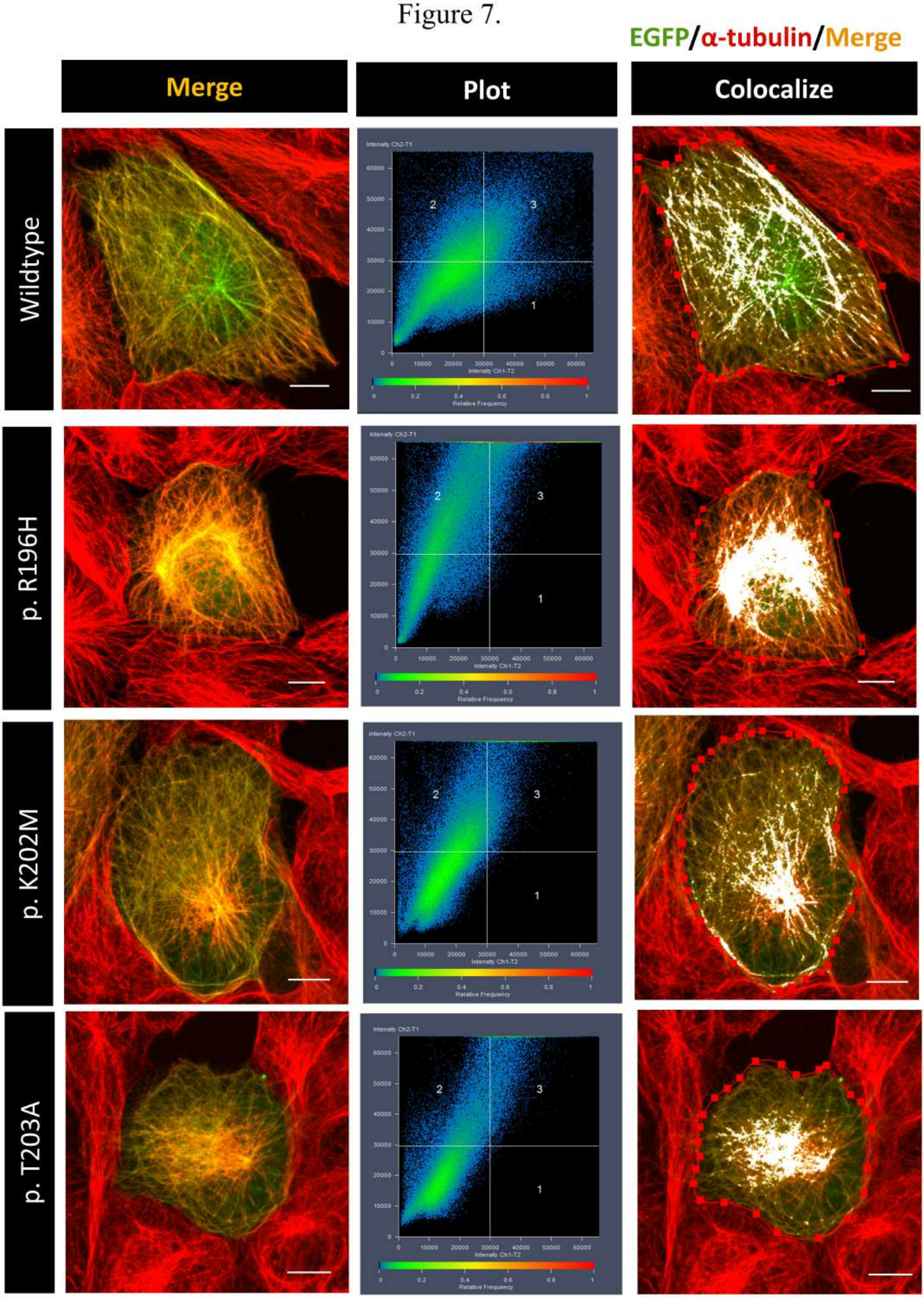
EGFP/α-tubulin/Merge
Merge
Plot
Colocalize
Wildtype
p. R196H
p. K202M
p. T203A
Intensity Ch2-T1
Intensity Ch1-T2
Relative Frequency
1
2
3

Figure 7.

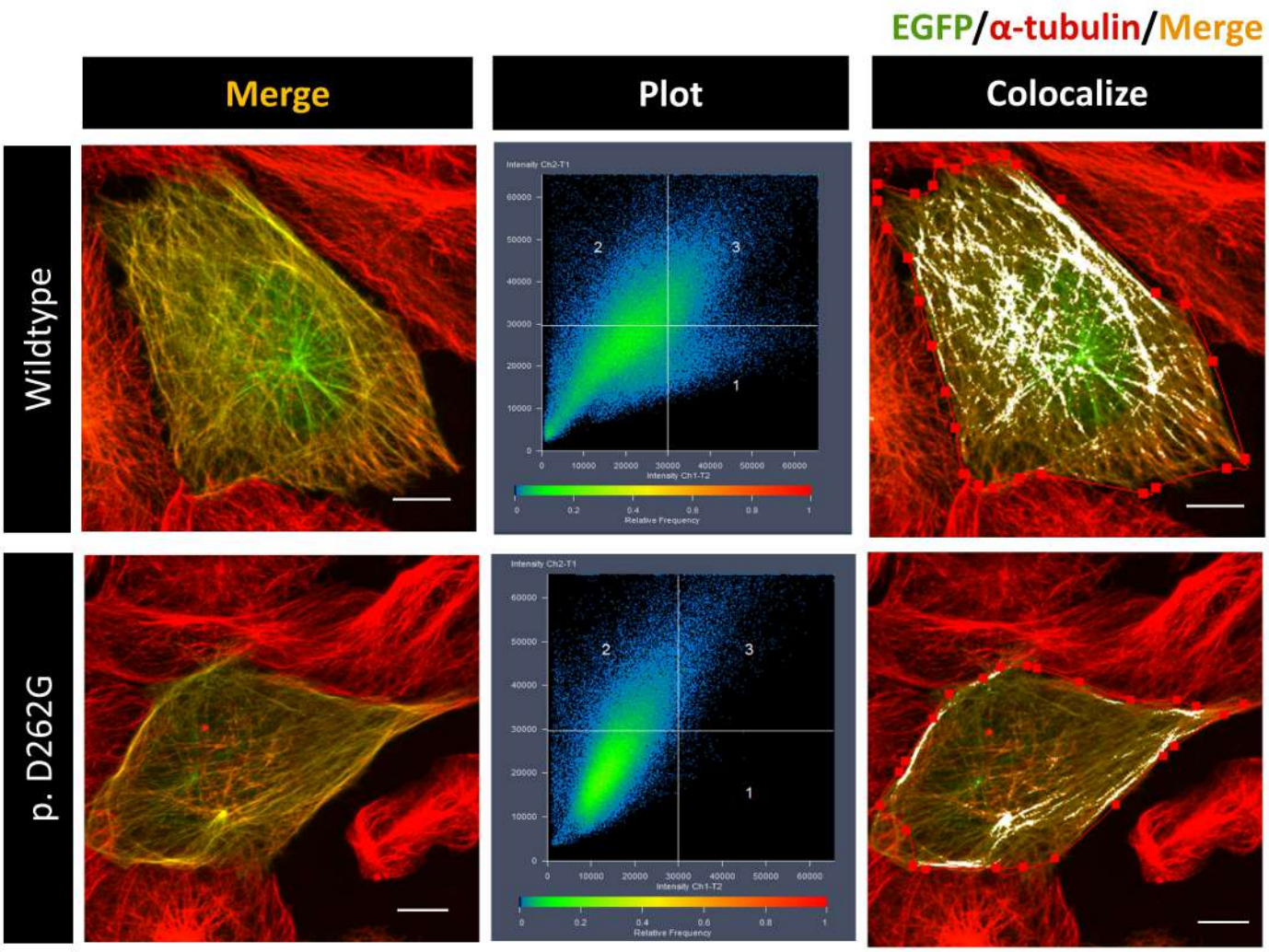
EGFP/α-tubulin/Merge
Merge
Plot
Colocalize
Wildtype
p. D262G
Intensity Ch2-T1
Intensity Ch1-T2
Relative Frequency
1
2
3

B.

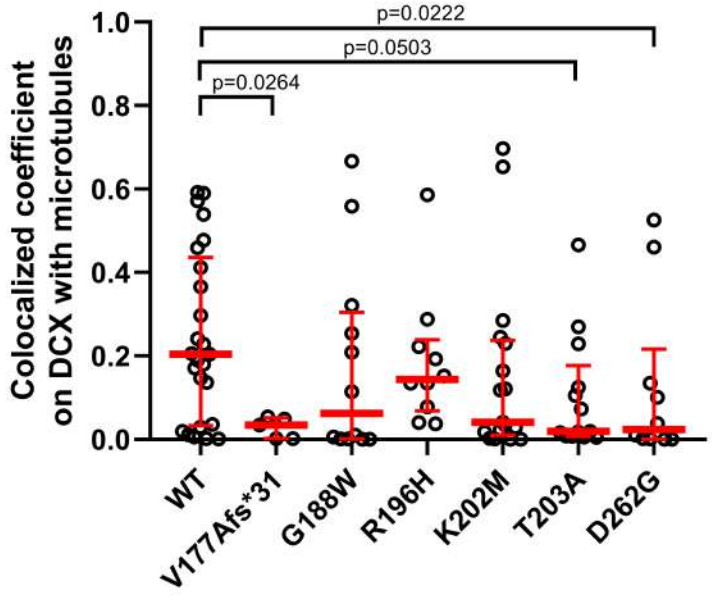
p=0.0222
p=0.0503
p=0.0264
Colocalized coefficient on DCX with microtubules
1.0
0.8
0.6
0.4
0.2
0.0
WT
V177Afs*31
G188W
R196H
K202M
T203A
D262G

Figure 7. DCX mutants defected the growing speed of microtubule till the stabilization stage.

(A) EGFP-DCX wild type or mutants were transfected in U2OS cells. Cold treating to lead microtubule entering into depolymerization and then recovered it back to growing stage at 37℃ for 10 minute. DCX p. V177Afs*31 cannot bind to microtubule properly, it would diffuse in cell cytoplasm. Other mutants still can see they can grow the microtubule but somehow there are some DCX mutants still in cytoplasm compared to wild type. It demonstrated that mutants cause the growing of microtubules slower. Thus, we used Zeiss colocalization analysis to calculate the coefficient between DCX and tubulins. Green signaling is EGFP-DCX wildtype or mutants, red signaling is α-tubulin, yellow signaling means DCX and α-tubulin co-localize together. The colocalization X-Y plane plot, X-bar is EGFP signaling while Y-bar is α-tubulin signaling. White plot is colocalized pixel. Scale bar: 10 μm.

(B) Quantification of colocalization coefficient on EGFP-DCX wildtype or mutants with tubulins. Median with interquartile range was shown on the data. Median number from wild type to p. D262G were 0.2040, 0.03400, 0.06200, 0.1435, 0.04100, 0.01900, 0.02400. DCX p.V177Afs*31 and p. D262G had significant differences while p. T203A had slightly changed.

Figure 8.

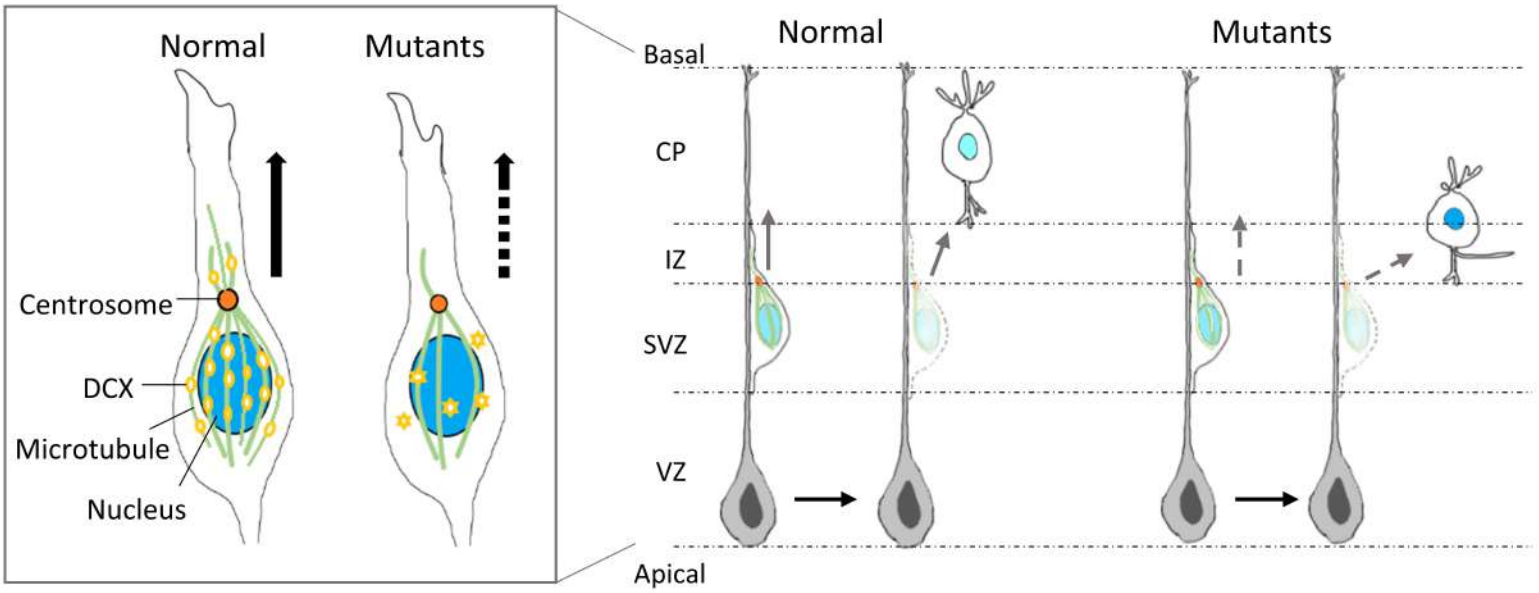

Figure 8. DCX mutants defected the formation of microtubules may delay the neuronal migration during brain development.

During somal translocation, microtubules form a "cage" formation surrounding the cell nucleus, and led to the brain cortex plate by centrosome. Thus, if DCX mutants defect the growing of microtubules, it may make neuronal migration delay and cause the brain developmental disorders. Mutations on DCX p. V177Afs*31, p. G188W, p. R196H, p. K202M and p. D262G might defect the brain development.

Figure S1.

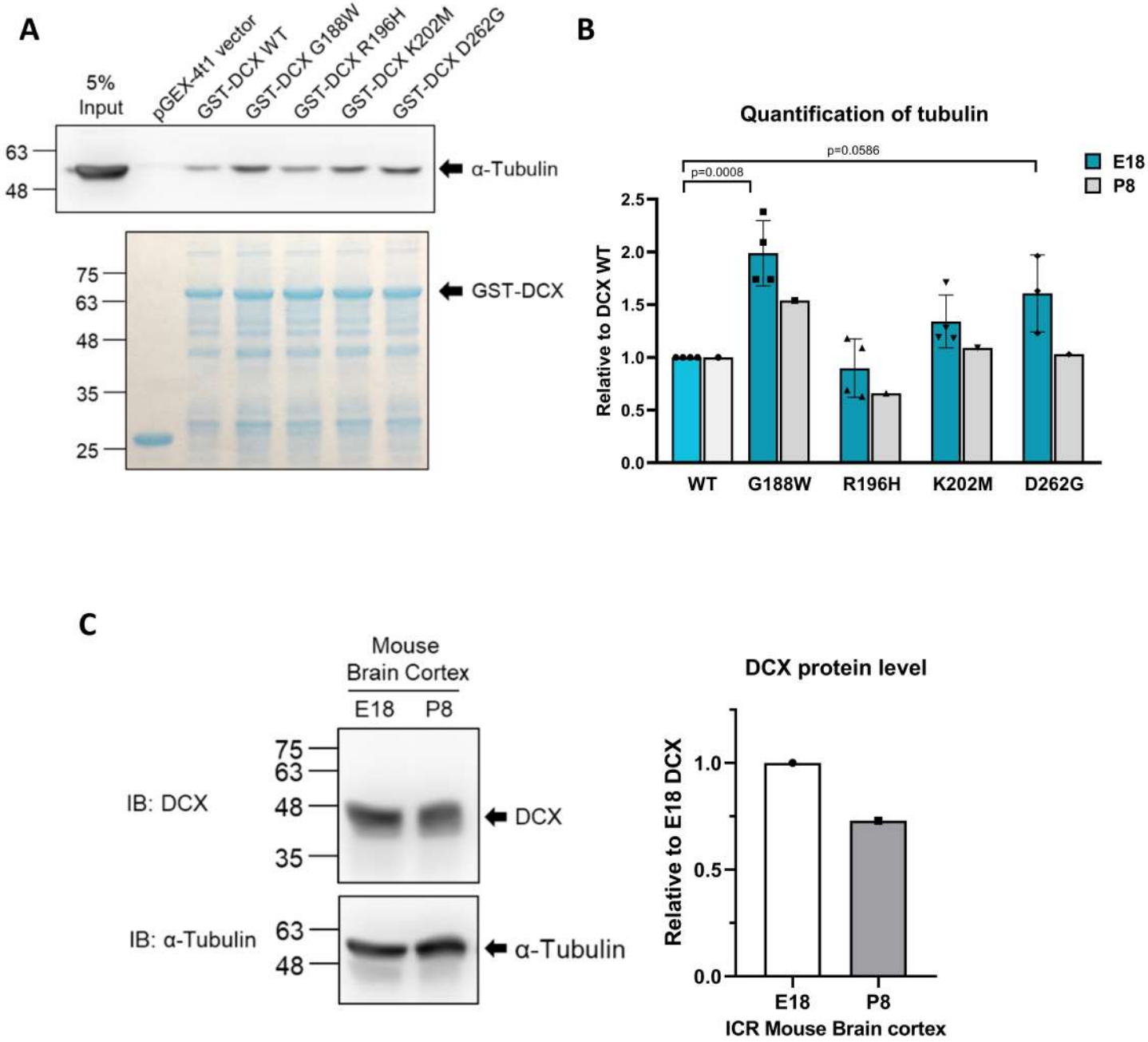
A
5% Input
pGEX-4t1 vector
GST-DCX WT
GST-DCX G188W
GST-DCX R196H
GST-DCX K202M
GST-DCX D262G
63
48
α-Tubulin
75
63
48
35
25
GST-DCX
B
Quantification of tubulin
p=0.0586
p=0.0008
E18
P8
Relative to DCX WT
2.5
2.0
1.5
1.0
0.5
0.0
WT
G188W
R196H
K202M
D262G
C
Mouse Brain Cortex
E18
P8
IB: DCX
75
63
48
35
DCX
IB: α-Tubulin
63
48
α-Tubulin
DCX protein level
Relative to E18 DCX
1.0
0.5
0.0
E18
P8
ICR Mouse Brain cortex

Figure S1. In vitro GST pull down assay on wild type doublecortin and the mutants.

(A) To see the interaction between microtubule and DCX wild type and mutants, E18/P8 mouse brain cortex was extracted and incubated with GST-DCX wild type or mutants. Input GST-DCX below was dyed with coomassie blue staining.

(B) It showed that DCX p. G188W (p=0.0008) and p. D262G (p=0.0586) might bind more E18 brain tubulins than wild type .

(C) DCX protein level in E18 and P8 mouse brain cortex. Protein level decreased in postnatal mice.

Figure S2.

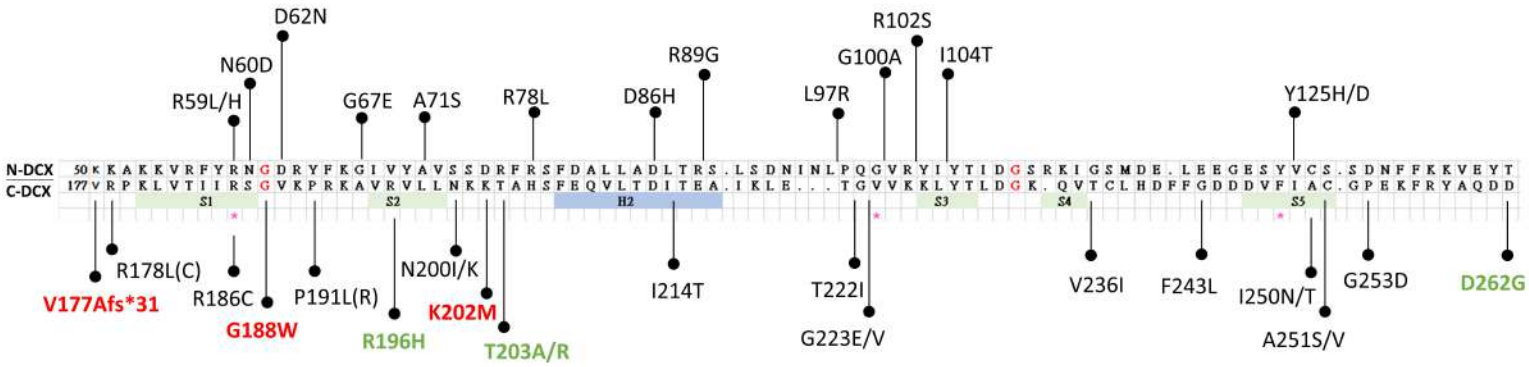

Figure S2. Similarity in N- and C-terminal binding domain of doublecortin.

In previous study, aligning with N- and C-terminal domain could find the similar three-dimensional fold (Kim et al., 2003). S1 to S5 are sheet-forming and H2 is helix-forming. Words in red means novel mutation, while in green are reported.

Figure S3.

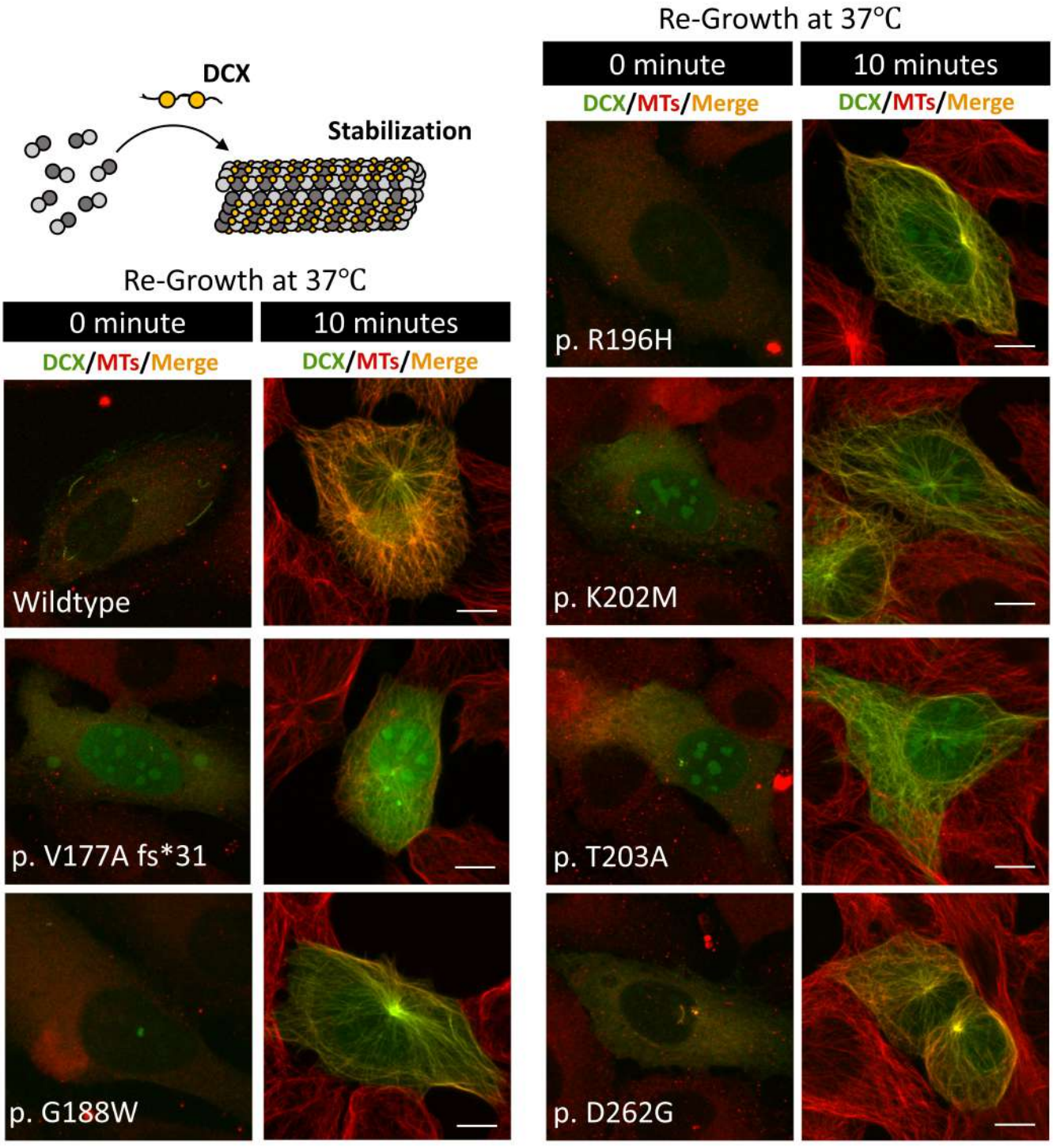
DCX
Stabilization
Re-Growth at 37°C
0 minute
10 minutes
DCX/MTs/Merge
DCX/MTs/Merge
Wildtype
p. V177A fs*31
p. G188W
Re-Growth at 37°C
0 minute
10 minutes
DCX/MTs/Merge
DCX/MTs/Merge
p. R196H
p. K202M
p. T203A
p. D262G

Figure S3. DCX mutations might delay microtubule growing in the stabilization stage.

EGFP-DCX wild type or mutants were introduced into U2OS cells, cold-treating them in 4˚C for 1 hour and recovering them at 37˚C. The time-point is 0 and 10 minutes, re-growing cells are shown on data. Microtubules depolymerized in cell cytoplasm at 0 minute, while microtubules grew back into stabilization at 10 minutes. Some EGFP signals still can see in cell cytoplasm compared to wild type. Green signal is EGFP-DCX wild type or mutants, red signal is α-tubulin. Scale bar: 10 μM.